INL/EXT-08-14847

Extended Forward Sensitivity Analysis for Uncertainty Quantification

Haihua Zhao
Vincent A. Mousseau

September 2008

The INL is a U.S. Department of Energy National Laboratory
operated by Battelle Energy Alliance

INL/EXT-08-14847

Extended Forward Sensitivity Analysis for Uncertainty Quantification

Haihua Zhao
Vincent A. Mousseau

September 2008

Idaho National Laboratory
Idaho Falls, Idaho 83415

http://www.inl.gov

Prepared for the
U.S. Department of Energy
Office of Nuclear Energy
Under DOE Idaho Operations Office
Contract DE-AC07-05ID14517

ABSTRACT

This report presents the forward sensitivity analysis method as a means for quantification of uncertainty in system analysis. The traditional approach to uncertainty quantification is based on a "black box" approach. The simulation tool is treated as an unknown signal generator, a distribution of inputs according to assumed probability density functions is sent in and the distribution of the outputs is measured and correlated back to the original input distribution. This approach requires large number of simulation runs and therefore has high computational cost. Contrary to the "black box" method, a more efficient sensitivity approach can take advantage of intimate knowledge of the simulation code. In this approach equations for the propagation of uncertainty are constructed and the sensitivity is solved for as variables in the same simulation. This "glass box" method can generate similar sensitivity information as the above "black box" approach with couples of runs to cover a large uncertainty region. Because only small numbers of runs are required, those runs can be done with a high accuracy in space and time ensuring that the uncertainty of the physical model is being measured and not simply the numerical error caused by the coarse discretization.

In the forward sensitivity method, the model is differentiated with respect to each parameter to yield an additional system of the same size as the original one, the result of which is the solution sensitivity. The sensitivity of any output variable can then be directly obtained from these sensitivities by applying the chain rule of differentiation. We extend the forward sensitivity method to include time and spatial steps as special parameters so that the numerical errors can be quantified against other physical parameters. This extension makes the forward sensitivity method a much more powerful tool to help uncertainty analysis. By knowing the relative sensitivity of time and space steps with other interested physical parameters, the simulation can be run at appropriate time and space steps that ensure numerical sensitivities will not affect the confidence of the physical parameter sensitivity results.

Two well defined benchmark problems, thermal wave and nonlinear diffusion, are utilized to demonstrate the extended forward sensitivity analysis method. All the physical solutions, parameter sensitivity solutions, even time step sensitivity in one case, have analytical forms, which allows the verification to be done in the strictest sense. A pilot code, Extended Forward sensitivity Analysis pilot code (EFA), has been developed to implement the above work.

CONTENTS

1. INTRODUCTION

Verification and validation (V&V) are playing more important roles to quantify uncertainties and realize high fidelity simulations in nuclear system analysis. Traditional V&V in nuclear system analysis more focus on the validation part or do not differentiate verification and validation. Progress in V&V in CFD fields [1] and from broader software engineering fields makes it possible to obtain high confidence in new high fidelity software. For example, order-of-accuracy verification in a 3-D CFD code has been performed through method of manufactured solution (MMS) [2] to verify second order accuracy and identify the existence of any first order errors. Advances in sensitivity analysis techniques [3, 4, 5, and 6] can be utilized to quantify uncertainties, which is meaningful only after rigorous V&V has guaranteed that the numerical errors are small.

The traditional approach [7, 8] to uncertainty quantification is based on a "black box" approach. The simulation tool is treated as an unknown signal generator, a distribution of inputs according to assumed probability density functions is sent in and the distribution of the outputs is measured and correlated back to the original input distribution. This approach is usually performed with coarse resolution models in space and time because of the larger number of simulation runs (say, 100) required to resolve the distribution of inputs. Even with coarse resolution models, the total computation cost of this method is still very high due to the requirement of many runs.

In contrast to the "black box" method, a more efficient sensitivity approach can take advantage of intimate knowledge of the simulation code. In this approach, equations for the propagation of uncertainty are constructed and the sensitivities are solved for as variables in the simulation. This can generate similar sensitivity information as the above "black box" approach with couples of runs to cover a large uncertainty region. Because only small numbers of runs are required, those runs can be done with a high accuracy in space and time ensuring that the uncertainty of the physical model is being measured and not simply the numerical error caused by the coarse discretization. Because of the increased efficiency and accuracy of this method, the uncertainty of many physical models can be measured and ordered according to uncertainty scales. Given this quantitative measure of uncertainty scales, one can prioritize the effort of model improvement according to where the model improvement will result in the largest reduction of uncertainty.

Two of the most popular sensitivity analysis methods are the forward sensitivity method and the adjoint sensitivity method [6, 9, 10, and 11]. In the forward sensitivity method, the model is differentiated with respect to each parameter to yield an additional system of the same size as the original one, the result of which is the solution sensitivity. The sensitivity of any output variable can then be directly obtained from these sensitivities by applying the chain rule of differentiation. The forward sensitivity method is most suitable when one needs the sensitivity information of many outputs with respect to relatively few parameters. In the adjoint method, the solution sensitivities need not be computed

explicitly. Instead, for each output variable of interest, one forms and solves an additional system, adjoint to the original one, the solution of which can then be used to evaluate the gradient of the output variable with respect to any set of model parameters. The adjoint sensitivity method is more practical than the forward approach when the number of parameters is large and when one needs the sensitivities of only few output variables [10, 11]. However, if one considers numerical errors important, extended forward sensitivity method with time step and spatial step as special parameters can be always applicable even for applications with large set of physical parameters.

This report only discusses forward sensitivity analysis methods. Two well defined benchmark problems are used to show and extend the technique. This work not only applies forward sensitivity analysis method with the strictest verification, but also extends the technique to include time and space step sensitivities as one method to quantify numerical errors. The report is organized in the following way: section 2 will present the basic forward sensitivity analysis theory; section 3 will discuss the Newton's method to solve nonlinear equations; section 4 will present how to estimate dynamical time and length scales which are important to select correct time and length steps; section 5 will present the first benchmark problem – thermal wave problem; section 6 will present the second benchmark problem – nonlinear diffusion problem; and the last section summary the conclusions and discuss further works.

2. FORWARD SENSITIVITY ANALYSIS

Consider the general form of a nonlinear system of partial differential equations

$$\frac{\partial \mathbf{Y}}{\partial t} - \mathbf{F}(t, \mathbf{Y}, p) = 0, \tag{2-1}$$

Here **Y** is the state vector, t time, **F** the vector of the functions, and p a parameter that the solution depends upon. We define the parameter sensitivity by how much it affects the solution or in equation form

$$\mathbf{s} = \frac{d\mathbf{Y}}{dp}, \tag{2-2}$$

Here **s** is the sensitivity of the solution **Y** with respect to the parameter p (we also call s_p as p parameter sensitivity).

The goal is to derive an equation for the time evolution of the sensitivity **s**:

$$\frac{\partial \mathbf{s}}{\partial t} = \frac{\partial}{\partial t}\frac{d\mathbf{Y}}{dp} = \frac{d}{dp}\frac{\partial \mathbf{Y}}{\partial t} = \frac{d\mathbf{F}}{dp}, \tag{2-3}$$

Here the first step made use of Eq. 2-2 and the second step employed Eq. 2-1. We now proceed to analyze the right hand side (RHS) of Eq. 2-3.

$$d\mathbf{F} = \frac{\partial \mathbf{F}}{\partial \mathbf{Y}} \partial \mathbf{Y} + \frac{\partial \mathbf{F}}{\partial t} \partial t + \frac{\partial \mathbf{F}}{\partial p} \partial p \,. \tag{2-4}$$

Therefore

$$\frac{d\mathbf{F}}{dp} = \frac{\partial \mathbf{F}}{\partial \mathbf{Y}} \frac{\partial \mathbf{Y}}{\partial p} + \frac{\partial \mathbf{F}}{\partial t} \frac{\partial t}{\partial p} + \frac{\partial \mathbf{F}}{\partial p} \frac{\partial p}{\partial p} = \frac{\partial \mathbf{F}}{\partial \mathbf{Y}} \mathbf{s} + \frac{\partial \mathbf{F}}{\partial p}, \tag{2-5}$$

From Eq. 2-2 and the fact that time is not a function of p. Combining Eqs. 2-3 and 2-5 we obtain the equation for the time evolution of the sensitivity **s**

$$\frac{\partial \mathbf{s}}{\partial t} = \frac{\partial \mathbf{F}}{\partial \mathbf{Y}} \mathbf{s} + \frac{\partial \mathbf{F}}{\partial p}. \tag{2-6}$$

We will simplify notation to describe the solution procedure. Define

$$\mathbf{f}(\mathbf{Y}) = \frac{\partial \mathbf{Y}}{\partial t} - \mathbf{F}(t, \mathbf{Y}, p), \tag{2-7}$$

$$\mathbf{g}(\mathbf{s}) = \frac{\partial \mathbf{s}}{\partial t} - \frac{\partial \mathbf{F}}{\partial \mathbf{Y}} \mathbf{s} - \frac{\partial \mathbf{F}}{\partial p}. \tag{2-8}$$

We will solve the nonlinear system of equations

$$\begin{bmatrix} \mathbf{f}(\mathbf{Y}) \\ \mathbf{g}(\mathbf{s}) \end{bmatrix} = 0, \tag{2-9}$$

using Newton's method. To solve this system we need the Jacobian matrix:

$$\mathbf{J} = \begin{bmatrix} \dfrac{\partial \mathbf{f}}{\partial \mathbf{Y}} & \dfrac{\partial \mathbf{f}}{\partial \mathbf{s}} \\ \dfrac{\partial \mathbf{g}}{\partial \mathbf{Y}} & \dfrac{\partial \mathbf{g}}{\partial \mathbf{s}} \end{bmatrix}. \tag{2-10}$$

We will now discuss each of the four components of Eq. 2-10. First we have

$$\tilde{\mathbf{J}} = \frac{\partial \mathbf{f}}{\partial \mathbf{Y}} = \frac{\partial}{\partial \mathbf{Y}} \left(\frac{\partial \mathbf{Y}}{\partial t} \right) - \frac{\partial \mathbf{F}}{\partial \mathbf{Y}}, \tag{2-11}$$

This is just the normal Jacobian matrix for solving Eq. 2-1 which we already have access from our Newton's solution method.

$$\frac{\partial \mathbf{f}}{\partial \mathbf{s}} = 0, \tag{2-12}$$

Since **f** does not depend on **s**.

$$\frac{\partial \mathbf{g}}{\partial \mathbf{s}} = \frac{\partial}{\partial \mathbf{s}} \left(\frac{\partial \mathbf{s}}{\partial t} \right) - \frac{\partial \mathbf{F}}{\partial \mathbf{Y}} = \tilde{\mathbf{J}}, \tag{2-13}$$

Since

$$\frac{\partial}{\partial \mathbf{Y}}\left(\frac{\partial \mathbf{Y}}{\partial t}\right)=\frac{\partial}{\partial \mathbf{s}}\left(\frac{\partial \mathbf{s}}{\partial t}\right), \tag{2-14}$$

when the same time discretization scheme is used for both the physical problem represented by Eq. 2-7 and the sensitivity problem represented by Eq. 2-8. To demonstrate this, one can use a first order time difference for both LHS and RHS terms:

$$\frac{\partial}{\partial \mathbf{Y}^{n+1}}\left(\frac{\mathbf{Y}^{n+1}-\mathbf{Y}^{n}}{\Delta t}\right)=\frac{1}{\Delta t}\cdot\mathbf{I}\ , \tag{2-15}$$

$$\frac{\partial}{\partial \mathbf{s}^{n+1}}\left(\frac{\mathbf{s}^{n+1}-\mathbf{s}^{n}}{\Delta t}\right)=\frac{1}{\Delta t}\cdot\mathbf{I}\ , \tag{2-16}$$

Where superscript n+1 and n represent time steps, Δt is the time step length, and **I** the identical matrix. Eq. 2-14 holds for other time difference schemes. The last step is to set

$$\frac{\partial \mathbf{g}}{\partial \mathbf{Y}}=0\,. \tag{2-17}$$

There are two reasons for this assumption. First the actual calculation of this derivative is very complicated. Second, it is safe to assume that the majority of the sensitivity comes from the physics which is in the normal Jacobian matrix so that the contribution from this derivative should be small. Either way, as long as the residuals defined by Eq. 2-9 are small, the corruption of the large Jacobian matrix by assuming $\frac{\partial \mathbf{g}}{\partial \mathbf{Y}}=0$ will only affect the convergence rate of the Jacobian iteration. It will not affect the accuracy of the solution of Eq. 2-9. So we can now write our Newton linearization as

$$\begin{bmatrix}\widetilde{\mathbf{J}} & \mathbf{0}\\ \mathbf{0} & \widetilde{\mathbf{J}}\end{bmatrix}\begin{bmatrix}\boldsymbol{\delta}\mathbf{Y}\\ \boldsymbol{\delta}\mathbf{s}\end{bmatrix}=-\begin{bmatrix}\mathbf{f(Y)}\\ \mathbf{g(s)}\end{bmatrix} \tag{2-18}$$

Eq. 2-18 will be iterated until the residual of Eq. 2-9 is small. Several researchers [4 and 5] tried to calculate $\frac{\partial \mathbf{g}}{\partial \mathbf{Y}}$, which ends up with a much more complex system to solve. We believe that ignoring $\frac{\partial \mathbf{g}}{\partial \mathbf{Y}}$ will allow the forward sensitivity method to be practical for large engineering system analysis applications.

Once we have solved for **Y** and **s** we can now plot the solution **Y** with uncertainty bars based on an uncertainty range in p defined as Δp,

$$\mathbf{Y}_{\pm}=\mathbf{Y}\pm\frac{d\mathbf{Y}}{dp}\Delta p=\mathbf{Y}\pm\mathbf{s}\Delta p\,. \tag{2-19}$$

There is an important assumption in using Eq. 2-19. This analysis requires that the truncation error in the solution method is small so that one is analyzing the physical model and not the numerical error. For this analysis the first step is to verify that the solution is not sensitive to the grid spacing Δx or time step Δt. This can be done through

two methods: the conventional time step and spatial step convergence study or taking Δx and Δt as special sensitivity parameters to calculate the solution sensitivities with them. The later method could be more efficient than conventional convergence study since they only require one run instead of series runs in convergence study. We will derive the methods to calculate Δx and Δt sensitivities in later sections.

3. NEWTON'S METHOD FOR NONLINEAR EQUATIONS

Newton's method [12, 13, and 14] is designed to solve nonlinear systems of the form:

$$\mathbf{res}(\mathbf{Y}) = 0\,, \tag{3-1}$$

Where **res** is the residue function vector for the discretized form of the nonlinear equations, like Eq. 2-9, and **Y** the solution variable vector. Newton's method solves Eq. 3-1 iteratively by solving a sequence of linear problems defined by:

$$\widetilde{\mathbf{J}}^{k}\boldsymbol{\delta}\mathbf{Y}^{k+1} = -\mathbf{res}(\mathbf{Y}^{k})\,, \tag{3-2}$$

Where the superscript "k" is the Newton iteration step index. The (i, j) element of the Jacobian matrix $\widetilde{\mathbf{J}}$ is the derivative of the ith residue equation with respect to the jth variable or in equation form:

$$\widetilde{J}(i,j) = \frac{\partial \mathbf{res}_i}{\partial \mathbf{Y}_j}. \tag{3-3}$$

The Jacobian matrix can be constructed analytically or by a numerical method:

$$\widetilde{J}_{i,j} \approx \frac{\mathbf{res}_i(\mathbf{Y} + \varepsilon \cdot \mathbf{e_j}) - \mathbf{res}_i(\mathbf{Y})}{\varepsilon}, \tag{3-4}$$

where ε is a small number, say 10^{-8} or calculated by more complex methods. $\mathbf{e_j}$ is a unit vector where all elements are zero except for the jth element, which is 1:

$$\mathbf{e_j} = [\delta_{1j}]\,. \tag{3-5}$$

Eq. 3-2 is solved for the update vector and then a new Newton iteration value for **Y** is computed from

$$\mathbf{Y}^{k+1} = \mathbf{Y}^{k} + \boldsymbol{\delta}\mathbf{Y}^{k+1}. \tag{3-6}$$

The iteration on **Y** is continued until the nonlinear residual given by Eq. 3-1 is small relative to its value for the initial guess:

$$\left\|\mathbf{res}(\mathbf{Y}^{k})\right\| < rtol \cdot \left\|\mathbf{res}(\mathbf{Y}^{0})\right\|, \tag{3-7}$$

or very small in its absolute value

$$\left\|\mathbf{res}(\mathbf{Y}^{k})\right\| < atol\,, \tag{3-8}$$

where rtol is the relative error tolerance, say 10^{-8}, and atoll is the absolute error tolerance, say 10^{-16}. Different norms can be used and we use L2-norm in this work for all the evaluation:

$$\|\mathbf{v}\|_2 = \sqrt{\sum_{i=1}^{n} \mathbf{v}_i^{\,2}}\,, \tag{3-9}$$

where **v** is any vector with n elements.

Calculating the sensitivity residual (Eq. 2-8) requires matrix and vector multiplication $\frac{\partial \mathbf{F}}{\partial \mathbf{Y}}\mathbf{s}$, which can be directly calculated by forming a matrix for $\frac{\partial \mathbf{F}}{\partial \mathbf{Y}}$ and doing the multiplication, or be avoided by numerical approximation, together with $\frac{\partial \mathbf{F}}{\partial p}$ [6]:

$$\frac{\partial \mathbf{F}}{\partial \mathbf{Y}}\mathbf{s} + \frac{\partial \mathbf{F}}{\partial p} = \frac{\mathbf{F}(t, \mathbf{Y} + \sigma \cdot \mathbf{s}, p + \sigma) - \mathbf{F}(t, \mathbf{Y} - \sigma \cdot \mathbf{s}, p - \sigma)}{2\sigma}, \tag{3-10}$$

Where σ is a small number, say 0.1% to 1% of p or calculated by more complex methods.

4. DYNAMICAL TIME AND SPACE SCALES

4.1 Dynamical Time Scale and Time Step Control

The appropriate time steps used in the solution methods should resolve the dynamic time scales of the physics in the problem [14]. Since the time scales in the problem are changing as the problem is evolving over time, an efficient algorithm would adjust the time step to adapt to the changing dynamic time scales. That means short time steps should be taken when the problem is changing rapidly while large time steps be taken when the problem is changing slowly.

Because of the implicit nature in Newton's methodology, there is no numerical stability limit and consequently the time step sizes can be determined based on the rate at which state variables change and the error control. The time step used here is called dynamical time step size control. The dynamical time scales for a generic state variable *y* is given by

$$\tau = \left(\left|\frac{1}{y}\frac{\partial y}{\partial t}\right|\right)^{-1}. \tag{4-1}$$

For a system that contains multiple equations in multiple variables and in multiple control volumes, a dynamical time scale is computed for each variable in each control volume. The time step is then based on the minimum of all the dynamical time scales for all control volumes.

The dynamical time scale for each variable in each control volume is approximated by

$$\tau_i^{n+1} = \left| \frac{0.5(y_i^n + y_i^{n-1})\Delta t^n}{y_i^n - y_i^{n-1}} \right|. \tag{4-2}$$

Taking the minimum across all control volumes and all variables, we obtain

$$\Delta t^{n+1} = \min[\tau_i^{n+1}, \alpha \Delta t^n], \tag{4-3}$$

where α controls the maximum rate at which the time step is allowed to grow.

4.2 Dynamical Spatial Scale

Similarly as for the time scale, a dynamical spatial scale can be calculated as

$$L = (\left| \frac{1}{y} \frac{\partial y}{\partial x} \right|)^{-1}. \tag{4-4}$$

The dynamical spatial scale for each variable in each control volume is approximated by

$$L_i^{n+1} = \left| \frac{0.5(y_{i-1}^n + y_i^n)\Delta x^n}{y_i^n - y_{i-1}^n} \right|. \tag{4-5}$$

Taking the minimum across all control volumes and all variables, we obtain

$$\Delta x^{n+1} = \min[L_i^{n+1}, \alpha \Delta x^n]. \tag{4-6}$$

5. THERMAL WAVE PROBLEM

5.1 Physical Model

We will first use the thermal wave problem [15, 16] as an example to investigate the forward sensitivity method. This problem has very useful analytical solutions for the problem itself and all the parameter sensitivities so that the numerical algorithms can be accurately verified. The following is the equation for the thermal wave problem:

$$\frac{\partial T}{\partial t} - \frac{\partial^2 T}{\partial x^2} = f(T), \tag{5-1}$$

for $x \in (-\infty, +\infty)$, and $t \geq 0$. We assume an exact solution which describes a thermal wave moving with a constant velocity c and with a constant wave width δ:

$$T(x,t,c,\delta) = \frac{1}{2}\left(1 - \tanh\left(\frac{x - ct}{\delta}\right)\right), \tag{5-2}$$

In Eq. 5-1, *f(T)* is the source term for the manufactured solution, which can be calculated by substituting an assumed solution T (Eq. 5-2) into the LHS of Eq. 5-1. The reference values for c and δ are: c=2, δ=1. In the later numerical analysis, we will limit the computation domain in [-10, 10]. Fig. 5-1 shows the analytical solution $T(x,t,c,\delta)$ (Eq.

5-2). The boundary conditions and initial condition will be directly derived from the analytical solution (Eq. 5-2).

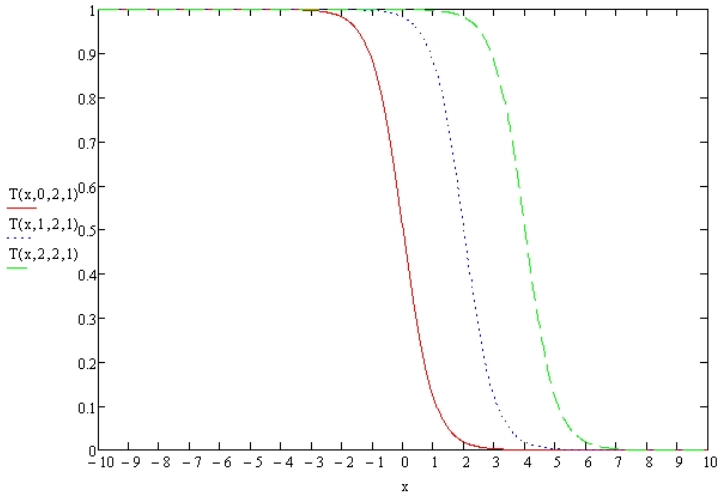

Figure 5-1: Analytical solution for the thermal wave problem.

Substitute Eq. 5-2 into the LHS of Eq. 5-1, we obtain:

$$f(T,c,\delta)=\frac{2T(1-T)(c\delta-2+4T)}{\delta^2}. \tag{5-3}$$

Fig. 5-2 shows the $f(x,t,c,\delta)$ function (Eq.5-3) for different time and with reference values for c and δ.

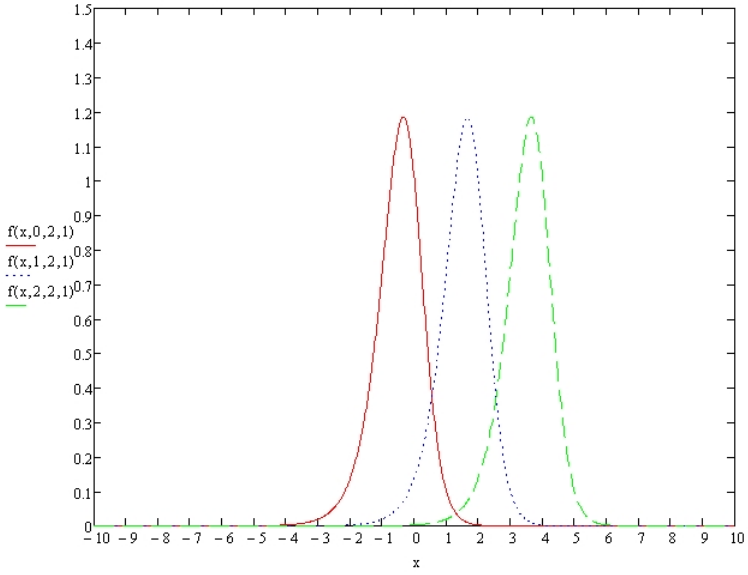

Figure 5-2: Source term for the thermal wave problem.

According to Eqs (4-1) and (4-4), the time scale and length scale can be derived as:

$$\tau_T(x,t,c,\delta) = \frac{\delta}{c\left(\tanh\left(\frac{x-ct}{\delta}\right)+1\right)}, \tag{5-4}$$

$$L_T(x,t,c,\delta) = \frac{\delta}{\tanh\left(\frac{x-ct}{\delta}\right)+1}. \tag{5-5}$$

We are only interested in the minimum scales, which can be easily derived according to Eqs. (5-4) and (5-5) as:

$$\tau_{T\min}(\delta) = \frac{\delta}{2c}, \tag{5-6}$$

$$L_{T\min}(c,\delta) = \frac{\delta}{2}. \tag{5-7}$$

These minimum scales will be used to select the maximum time step and spatial steps in numerical calculations shown in later sections.

With the analytical solution Eq.5-2, the solution sensitivity with respective to parameter c,

$$s_c = \frac{dT}{dc}, \tag{5-8}$$

and the solution sensitivity with respective to the parameter δ,

$$s_\delta = \frac{dT}{d\delta}, \tag{5-9}$$

can be easily derived as:

$$s_c(x,t,c,\delta) = \frac{1}{2}\left(1-\tanh\left(\frac{x-ct}{\delta}\right)^2\right)\frac{t}{\delta}, \tag{5-10}$$

$$s_\delta(x,t,c,\delta) = \frac{1}{2}\left(1-\tanh\left(\frac{x-ct}{\delta}\right)^2\right)\left(\frac{x-ct}{\delta^2}\right), \tag{5-11}$$

Figs. 5-3 and 5-4 show the analytical parameter sensitivity solutions $s_c(x,t,c,\delta)$ (Eq. 5-10) and $s_\delta(x,t,c,\delta)$ (Eq. 5-11), respectively.

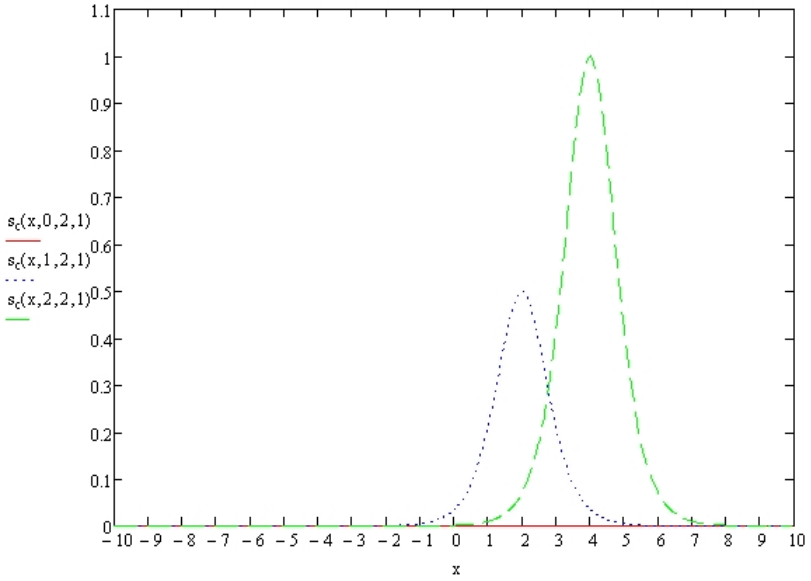

Figure 5-3: Analytical solution for the sensitivity s_c.

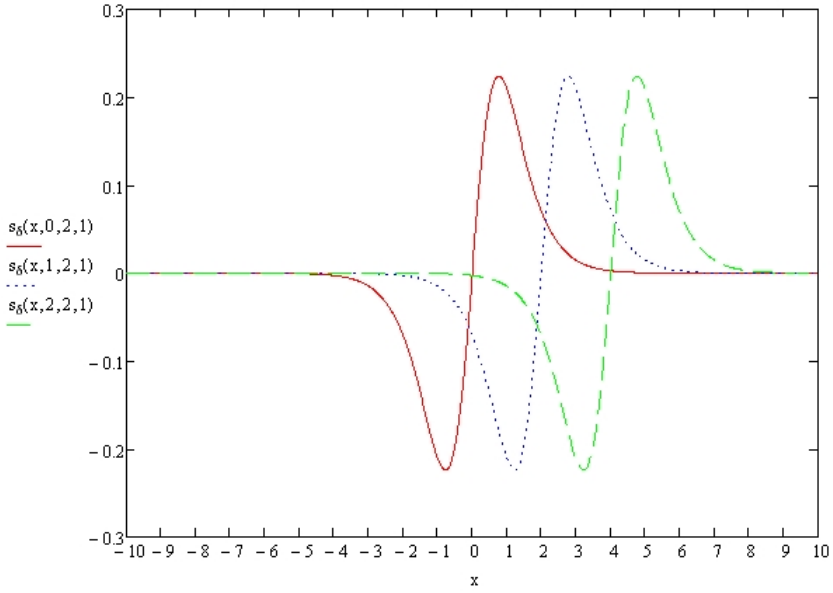

Figure 5-4: Analytical solution for the sensitivity s_δ.

The time scale for s_c is:

$$\tau_{s_c}(x,t,c,\delta) = \frac{\delta \cdot t}{\delta + 2c \cdot t \cdot \tanh\left(\frac{x-ct}{\delta}\right)}. \tag{5-12}$$

The minimum time scale for s_c is:

$$\tau_{s_c \min}(t,c,\delta) = \frac{\delta \cdot t}{\delta + 2c \cdot t}, \tag{5-13}$$

We note that:

$$\tau_{s_c \min}(t \to 0,c,\delta) = 0, \tag{5-14}$$

$$\tau_{s_c \min}(t \to \infty,c,\delta) = \frac{\delta}{2c}. \tag{5-15}$$

The length scale for s_c is:

$$L_{s_c}(x,t,c,\delta) = \frac{\delta}{2\tanh\left(\frac{x-ct}{\delta}\right)}. \tag{5-16}$$

The minimum length scale for s_c is:

$$L_{s_c \min}(\delta) = \frac{\delta}{2}. \tag{5-17}$$

The time scale for s_δ is:

$$\tau_{s_\delta}(x,t,c,\delta) = \left| \frac{x-ct}{c\left(1 - 2 \cdot \frac{x-ct}{\delta} \cdot \tanh\left(\frac{x-ct}{\delta}\right)\right)} \right|. \tag{5-18}$$

The minimum time scale for s_δ in the computational domain is 0 when $t < 10/c$. The length scale for s_δ is:

$$L_{s_\delta}(x,t,c,\delta) = \left| \frac{x-ct}{1 - 2 \cdot \frac{x-ct}{\delta} \cdot \tanh\left(\frac{x-ct}{\delta}\right)} \right|. \tag{5-19}$$

The minimum length scale for s_δ in the computational domain is 0 when $t < 10/c$.

For the solution sensitivities with respective to the time step and the spatial step, one can not directly derive the sensitivity equations from the original PDEs since the time and spatial steps are discrete quantities that depend on the discretization method. Let's consider the time step sensitivity. When we discretize a PDE, the actual discrete equation to be solved is the original PDE with added local truncation error. If we subtract the local truncation error term in the PDE, the modified equation will give us a higher order solution. For the first order backward Euler scheme, the local truncation error term is

$$LTE_t = \frac{\Delta t}{2}\frac{\partial^2 T}{\partial t^2}, \tag{5-20}$$

and the modified equation is

$$\frac{\partial T}{\partial t} - \frac{\partial^2 T}{\partial x^2} - \frac{\Delta t}{2}\frac{\partial^2 T}{\partial t^2} = f(T). \tag{5-21}$$

We will derive time step sensitivity equation according to Eq. 5-21 and Eq. 2-8. Rick Rauenzahn at Los Alamos National Laboratory (LANL) derived the analytical solution for Eq. 5-21 for the reference values of c=2 and δ=1:

$$T_{MEA}(x,t,\Delta t) = \frac{1}{2}\left(1 - \tanh\left(\frac{x - \frac{2}{\sqrt{1-2\Delta t}}t}{\frac{1}{\sqrt{1-2\Delta t}}}\right)\right). \tag{5-22}$$

According to this equation, we can derive an analytical solution for time step sensitivity for the 1st order backward Euler scheme:

$$s_{\Delta t}(x,t,\Delta t) = \frac{x\left(1 - \tanh\left(x\sqrt{1-2\Delta t} - 2t\right)^2\right)}{2\sqrt{1-2\Delta t}}. \tag{5-23}$$

Fig. 5-5 shows $s_{\Delta t}(x,t,\Delta t)$ for three different times with a fixed time step and Fig. 5-6 shows the $s_{\Delta t}(x,t,\Delta t)$ for five different time steps at the same time. Fig. 5-5 shows the solution sensitivity with respective to the time step increases with time and reflects the accumulation of local truncation error over time. One interesting result according to Fig. 5-6 and Eq. 5-23 is that the time step sensitivities for smaller time steps converge to one solution.

The time scale for $s_{\Delta t}$ is:

$$\tau_{s_{\Delta t}}(x,t,\Delta t) = \left|\frac{1}{4\tanh(2t - x\sqrt{1-2\Delta t})}\right|. \tag{5-24}$$

The minimum time scale for $s_{\Delta t}$ is ¼. The length scale for $s_{\Delta t}$ is:

$$L_{s_{\Delta t}}(x,t,\Delta t) = \left|\frac{x}{1 + 2x\cdot\sqrt{1-2\Delta t}\cdot\tanh(2t - x\sqrt{1-2\Delta t})}\right|. \tag{5-25}$$

The minimum length scale for $s_{\Delta t}$ is 0.

For other time step schemes, local truncation errors can be derived and the time step sensitivity can be numerically solved. So this is a generic method to consider time step errors. The time step sensitivity here reflects the accumulated time step error instead of local errors. The accumulated time step error usually cannot be obtained except for special cases with analytical solutions. The spatial step sensitivity equation can be

derived with a similar method. Since for the thermal wave problem, we need a fourth order partial differential term for the spatial step truncation error, and we don not have an analytical solution for the modified equation. Therefore, we leave this investigation for other problems which have more easier modified equations.

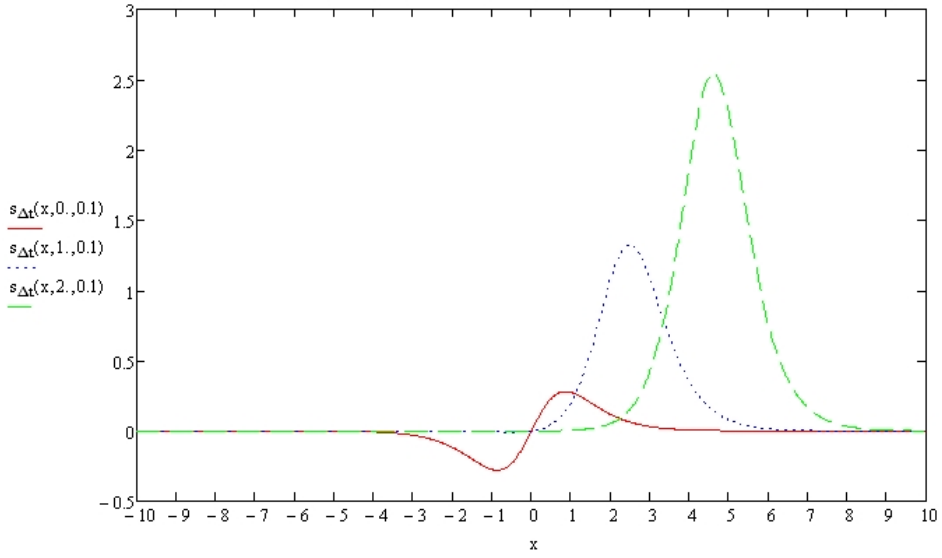

Figure 5-5: Analytical solution for the sensitivity $s_{\Delta t}$ for different times.

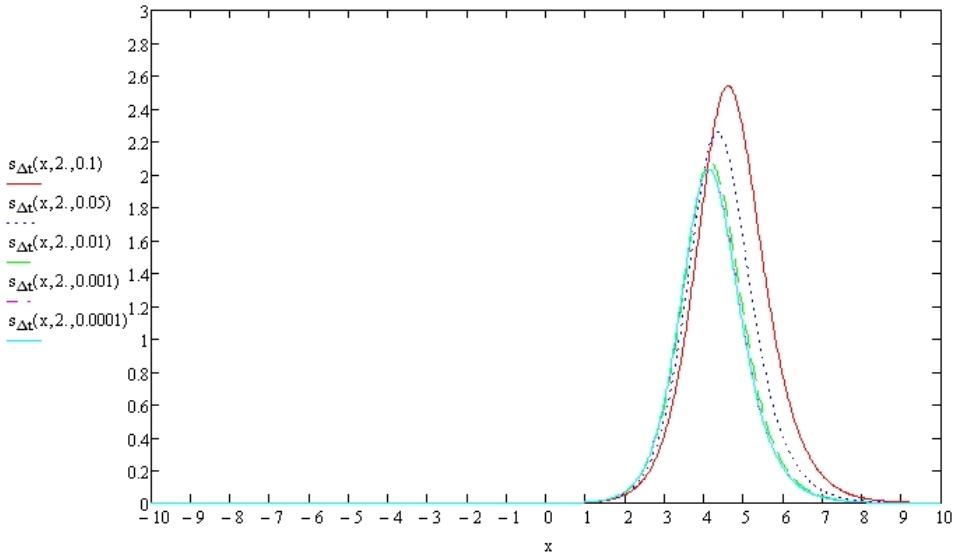

Figure 5-6: Analytical solution for the sensitivity $s_{\Delta t}$ for different time steps.

5.2 Numerical Models

We use Newton's method to solve the physical problem defined by Eq. 5-1 with exact boundary conditions and the initial condition according to Eq. 5-2, and the associated sensitivity problems. Note that for each time step, according to Eq. 2-18, the physical problem can be solved first and all the sensitivity equations can then be solved later in parallel. If the sensitivity parameters are numerous, each sensitivity equation can be solved on separate CPUs. This natural parallel structure will greatly facilitate the use of super computers.

F function in Eq. 5-1 for the physical problem and associated sensitivity problems (s_c and s_δ) as described by Eq. 2-7 and Eq. 2-8 is,

$$F(x,t,T,c,\delta)=\frac{\partial^2 T}{\partial x^2}+f(T,c,\delta). \tag{5-26}$$

For time step sensitivity problem, the corresponding function is,

$$F(x,t,T,c,\delta,\Delta t)=\frac{\partial^2 T}{\partial x^2}+\frac{\Delta t}{2}\frac{\partial^2 T}{\partial t^2}+f(T,c,\delta). \tag{5-27}$$

The discretized nonlinear residual equation for the physical problem at time step n+1 and control volume (CV) i is written as

$$res_i(\mathbf{T}^{n+1})=\frac{T_i^{n+1}-T_i^n}{\Delta t}-\theta\cdot F^{n+1}-(1-\theta)\cdot F^n, \tag{5-28}$$

where $res_i(\mathbf{T}^{n+1})$ represents the ith element in the residual vector and θ is a parameter to control the implicitness of the numerical schemes, for example,

$$\theta=\begin{cases}1, & \text{first order fully implicit method (backward Euler)}\\ 0.5, & \text{second order Crank - Nicolson method (C - N)}\\ 0, & \text{first order explicit method}\end{cases} \tag{5-29}$$

The diffusion term can be discretized with the central difference method:

$$\left.\frac{\partial^2 T}{\partial x^2}\right|_i=\frac{1}{\Delta x^2}\left(T_{i+1}+T_{i-1}-2T_i\right) \qquad for \quad i=2,...,I-1, \tag{5-30}$$

where subscript i represents the spatial control volume index. Note that the solution value is located at the center of each control volume. For the first type of boundary conditions, the boundary values (i=0 or i=I+1) are located at the boundary of the control volume. Therefore Eq. (5-30) needs to be adjusted to reflect the fact of zero width control volumes. We can derive the 2nd order discrete forms for CV 1 and CV I with the Taylor expansion method as:

$$\frac{\partial^2 T}{\partial x^2}_1 = \frac{1}{\Delta x^2}\left(\frac{4}{3}T_2 + \frac{8}{3}T_0 - 4T_1\right), \tag{5-31}$$

$$\frac{\partial^2 T}{\partial x^2}_I = \frac{1}{\Delta x^2}\left(\frac{8}{3}T_{I+1} + \frac{4}{3}T_{I-1} - 4T_I\right). \tag{5-32}$$

Two different methods are used to form the problem residue Jacobian matrix defined by Eq. 3-3. The first one uses direct evaluation method as defined by Eq. 3-3 and the second one uses approximate method defined by Eq. 3-4. Note that the Jacobian matrix is tridiagonal in this 1-D problem:

$$\widetilde{\mathbf{J}} = tridiag(\widetilde{J}_{i,i-1}, \widetilde{J}_{i,i}, \widetilde{J}_{i,i+1}). \tag{5-33}$$

According to Eqs. 3-3, 5-28, 5-26, 5-30, 5-31, and 5-32, direct evaluation Jacobian matrix inputs are:

$$\widetilde{J}_{i,i-1} = \frac{\partial res_i(\mathbf{T}^{n+1})}{\partial T_{i-1}^{n+1}} = -\frac{\theta}{\Delta x^2} \qquad for \quad i = 2,...,I-1 \tag{5-34}$$

$$\widetilde{J}_{I,I-1} = \frac{\partial res_I(\mathbf{T}^{n+1})}{\partial T_{I-1}^{n+1}} = -\frac{4}{3}\frac{\theta}{\Delta x^2} \tag{5-35}$$

$$\widetilde{J}_{i,i} = \frac{\partial res_i(\mathbf{T}^{n+1})}{\partial T_i^{n+1}} = \frac{1}{\Delta t} + \frac{2\theta}{\Delta x^2} + \frac{2\theta}{\delta^2}\left[12\left(T_i^{n+1}\right)^2 + (2\delta c - 12)T_i^{n+1} + 2 - \delta c\right] \qquad for \quad i = 2,...,I-1 \tag{5-36}$$

$$\widetilde{J}_{1,1} = \frac{\partial res_1(\mathbf{T}^{n+1})}{\partial T_1^{n+1}} = \frac{1}{\Delta t} + \frac{4\theta}{\Delta x^2} + \frac{2\theta}{\delta^2}\left[12\left(T_1^{n+1}\right)^2 + (2\delta c - 12)T_1^{n+1} + 2 - \delta c\right] \tag{5-37}$$

$$\widetilde{J}_{I,I} = \frac{\partial res_I(\mathbf{T}^{n+1})}{\partial T_I^{n+1}} = \frac{1}{\Delta t} + \frac{4\theta}{\Delta x^2} + \frac{2\theta}{\delta^2}\left[12\left(T_I^{n+1}\right)^2 + (2\delta c - 12)T_I^{n+1} + 2 - \delta c\right] \tag{5-38}$$

$$\widetilde{J}_{i,i+1} = \frac{\partial res_i(\mathbf{T}^{n+1})}{\partial T_{i+1}^{n+1}} = -\frac{\theta}{\Delta x^2} \qquad for \quad i = 2,...,I-1 \tag{5-39}$$

$$\widetilde{J}_{1,2} = \frac{\partial res_1(\mathbf{T}^{n+1})}{\partial T_2^{n+1}} = -\frac{8}{3}\frac{\theta}{\Delta x^2} \tag{5-40}$$

According to Eqs. 3-4 and 5-28, the Jacobian matrix can also be approximately obtained by:

$$\widetilde{J}_{i,i-1} = \frac{\partial res_i(\mathbf{T}^{n+1})}{\partial T_{i-1}^{n+1}} \approx \frac{res_i(\mathbf{T}^{n+1} + \varepsilon \cdot \mathbf{e_{i-1}}) - res_i(\mathbf{T}^{n+1})}{\varepsilon} \qquad for \quad i = 2,...,I, \tag{5-41}$$

$$\widetilde{J}_{i,i} = \frac{\partial res_i(\mathbf{T}^{n+1})}{\partial T_i^{n+1}} \approx \frac{res_i(\mathbf{T}^{n+1} + \varepsilon \cdot \mathbf{e_i}) - res_i(\mathbf{T}^{n+1})}{\varepsilon} \quad , \quad for \quad i = 1,...,I \tag{5-42}$$

$$\widetilde{J}_{i,i+1} = \frac{\partial res_i(\mathbf{T}^{n+1})}{\partial T_{i+1}^{n+1}} \approx \frac{res_i(\mathbf{T}^{n+1} + \varepsilon \cdot \mathbf{e_{i+1}}) - res_i(\mathbf{T}^{n+1})}{\varepsilon} \quad . \quad for \quad i = 1,...,I-1 \tag{5-43}$$

For the sensitivity problem, the same Jacobian matrix is used as for the physical problem. The discretized residual function for the sensitivity problem is:

$$ress_i(\mathbf{s}^{n+1}) = \frac{s_i^{n+1} - s_i^n}{\Delta t} - \theta \cdot \left(\frac{\partial F}{\partial Y} s + \frac{\partial F}{\partial p} \right)_i^{n+1} - (1-\theta) \cdot \left(\frac{\partial F}{\partial Y} s + \frac{\partial F}{\partial p} \right)_i^{n} . \tag{5-44}$$

Although it is possible to directly evaluate the $\frac{\partial F}{\partial Y} s + \frac{\partial F}{\partial p}$ term, the form becomes very complex and error-prone due to the matrix-vector multiplication $\frac{\partial F}{\partial Y} s$ and directly deriving $\frac{\partial F}{\partial p}$. This term can be approximated by the second order Jacobian free method (Eq. 3-10) as

$$\left(\frac{\partial F}{\partial Y} s + \frac{\partial F}{\partial p} \right)_i = \frac{F_i(x,t,\mathbf{T} + \sigma \cdot \mathbf{s}, p + \sigma) - F_i(x,t,\mathbf{T} - \sigma \cdot \mathbf{s}, p - \sigma)}{2\sigma} . \tag{5-45}$$

For the sensitivity problem for Δt, the first term in $\frac{\partial F}{\partial Y} s + \frac{\partial F}{\partial p}$ can be approximated by the following equation:

$$\left(\frac{\partial F}{\partial Y} \mathbf{s}_{\Delta \mathbf{t}} \right)_i = \frac{F_i(x,t,\mathbf{T} + \sigma \cdot \mathbf{s}_{\Delta \mathbf{t}}) - F_i(x,t,\mathbf{T} - \sigma \cdot \mathbf{s}_{\Delta \mathbf{t}})}{2\sigma} , \tag{5-46}$$

where F is according to Eq. (5-26) without adding the local time step truncation term; the second term is analytically derived according to Eq. (5-27):

$$\left(\frac{\partial F}{\partial \Delta t} \right)_i = \left(\frac{1}{2} \frac{\partial^2 T}{\partial t^2} \right)_i \approx \frac{1}{2\Delta t^2} \left(T_i^{n+1} + T_i^{n-1} - 2T_i^n \right). \tag{5-47}$$

Similar treatment for Δx sensitivity residue can be constructed. However due to its higher order nature in this particular problem, we will leave it to other simpler problems.

5.3 Numerical Results

This section will first show the results of convergence studies for both time and space, and for both the physical problem and associated parameter sensitivity problems. Then a special discussion will be given for the Δt sensitivity results. Since we have analytical solutions for the thermal wave problem and all the parameter sensitivities, we can accurately calculate the absolute error according to the following equation [1]:

$$err_{abs} = \frac{\left\| \mathbf{v}_{numerical} - \mathbf{v}_{analytical} \right\|_2}{\sqrt{n}}, \tag{5-48}$$

Here n is the number of control volumes. Finally an example will be given to show how to use the sensitivity information by considering the numerical error from the time step integration.

Both analytical Jacobian matrix (Eq. 5-34 to Eq. 5-40) and the numerical Jacobian matrix (Eq. 5-41 to Eq. 5-43) were tested. The convergence speeds for both methods are very fast. To reduce computation cost, the analytical Jacobian is used for all the later calculations.

5.3.1 Convergence Study for the Physical Problem

First we consider a convergence study for the physical problem. Fig. 5-7 shows the space convergence study for C-N scheme with very small time step ($\Delta t = 10^{-4}$). Except for the first two large Δx values which are larger than the minimum dynamical length scale (0.5, according to Eq. 5-7), the subsequent errors drop by about 4 times when Δx is halved, which clearly shows the 2nd order spatial step convergence rate. Fig. 5-8 shows the time convergence study for C-N scheme with small spatial step ($\Delta x = 1/32$). The solution errors drop approximately by 4 times when Δt is halved until the spatial error dominates the total error, which proves the 2nd order time step convergence rate. Fig. 5-9 shows the time convergence study for 1st order backward Euler scheme with small spatial step ($\Delta x = 1/32$). The solution errors drop approximately by half when Δt is halved, which shows the 1st order convergence rate. The spatial convergence rate is still 2nd order even for the 1st order time scheme.

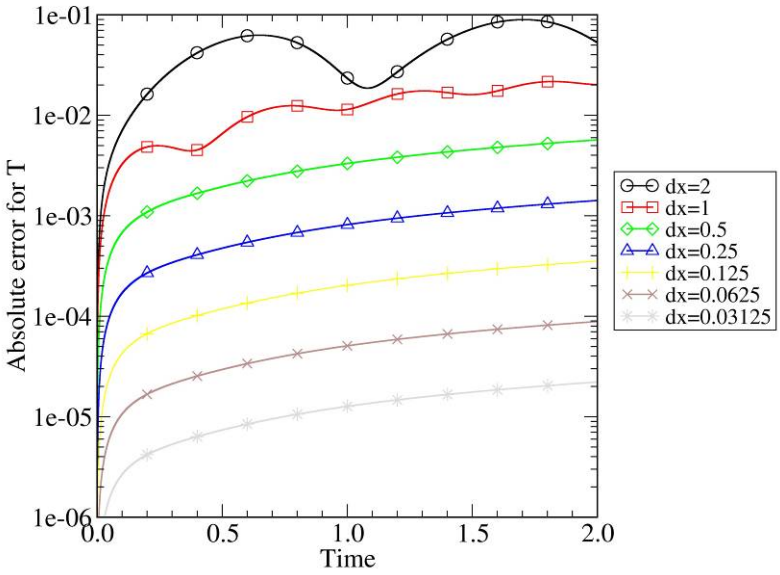

Figure 5-7: Space convergence study for the thermal wave problem, C-N scheme, $\Delta t = 10^{-4}$.

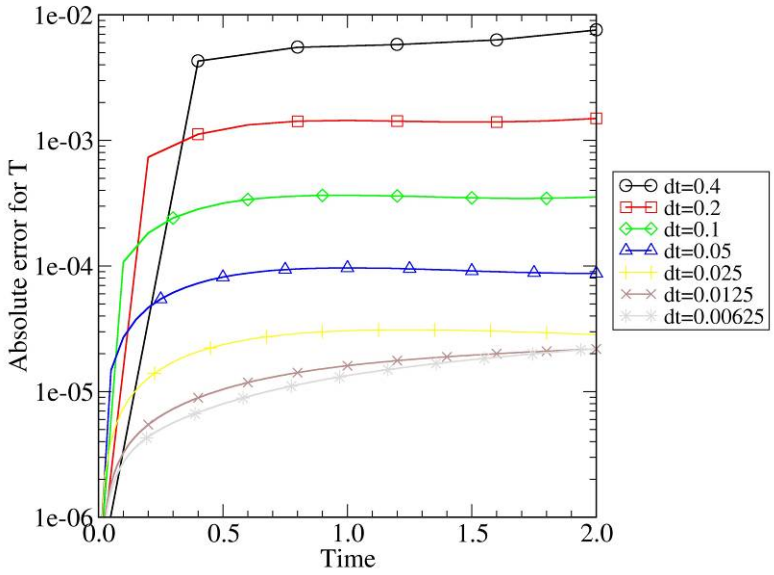

Figure 5-8: Time convergence study for the thermal wave problem, C-N scheme, $\Delta x = 1/32$.

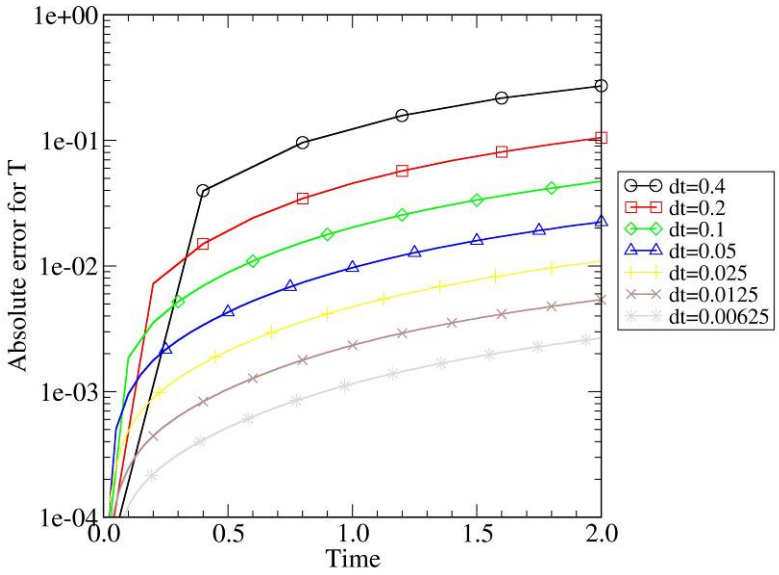

Figure 5-9: Time convergence study for the thermal wave problem, backward Euler scheme, Δx =1/32.

5.3.2 Convergence Study and Results for s_c and s_δ

Both time and space convergence studies for the parameter sensitivities were performed. Through numerical experiments, we found both the relative and absolute error tolerances in Newton iteration (Eq. 3-7 and 3-8) need to be relaxed in order to converge for the sensitivity equations, i.e., increasing by 100 times than the values for the physical problem itself. Although we use the physical problem Jacobian to approximate the sensitivity problem Jacobian, the total Newton iteration numbers for sensitivity problems are close to the iteration number needed for solving the physical problem itself. Therefore, the CPU time needed to solve sensitivity problems is proportional to the number of sensitivities.

Fig. 5-10 shows the space convergence study for the sensitivity s_c for C-N scheme with very small time step ($\Delta t = 10^{-4}$). For Δx larger than the minimum dynamical length scale, we observe there exists oscillation behavior with time; For smaller Δx, other errors due to the approximation treatment on sensitivity residue (Eq. 5-45), Newton iteration convergence control tolerance, and time step error begin to dominate so that the convergence speed becomes lower and finally stopped. For the middle range of Δx between 0.5 to 0.125, 2nd order convergence speed is apparent. Fig. 5-11 shows the time convergence study for the sensitivity s_c for C-N scheme with a small spatial step (Δx =1/32). 2nd order convergence speed is achieved until Δt becomes too small when other errors similar as shown in the space convergence study begin to dominate. Fig. 5-12 shows the time convergence study for the sensitivity s_c for the 1st order backward Euler scheme with a small spatial step (Δx =1/32). It is very clear that the 1st order convergence speed is obtained.

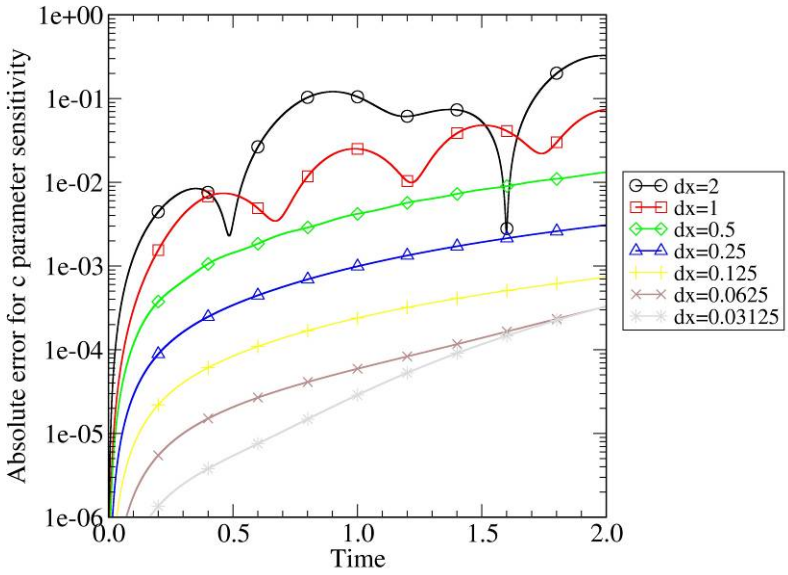

Figure 5-10: Space convergence study for the sensitivity s_c in the thermal wave problem, C-N scheme, $\Delta t = 10^{-4}$.

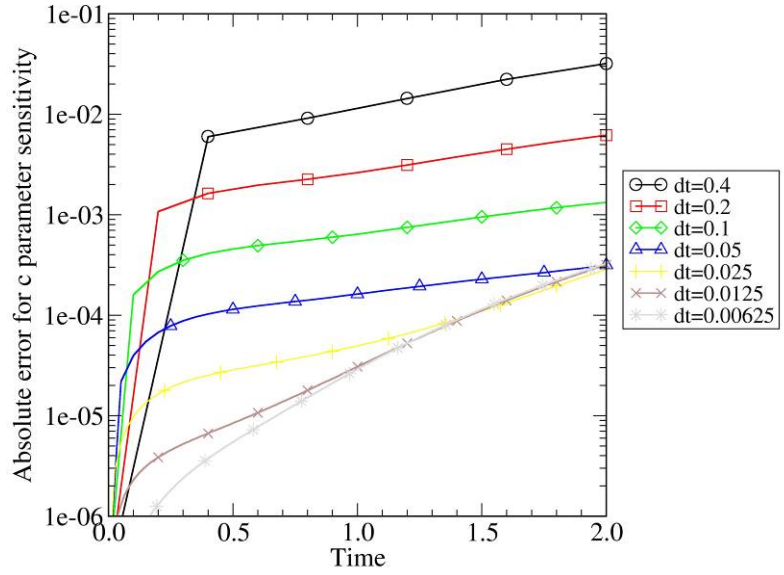

Figure 5-11: Time convergence study for the sensitivity s_c in the thermal wave problem, C-N scheme, $\Delta x = 1/32$.

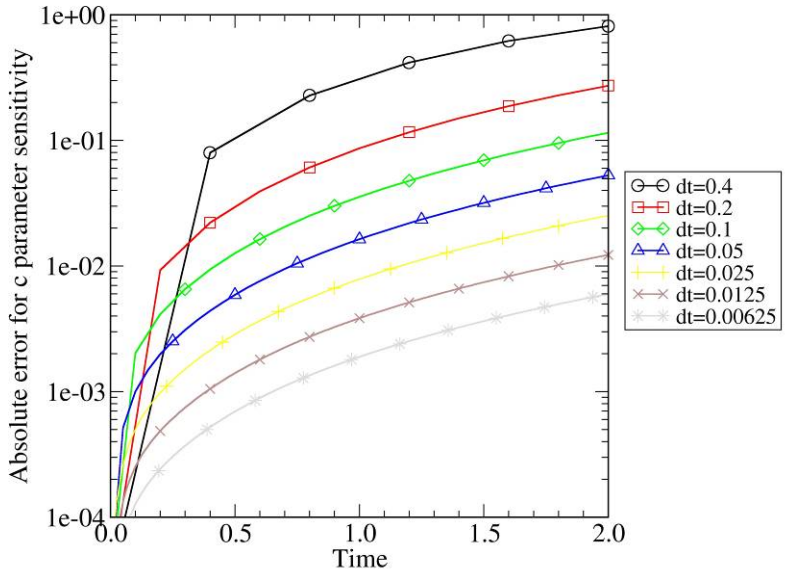

Figure 5-12: Time convergence study for the sensitivity s_c in the thermal wave problem, backward Euler scheme, Δx =1/32.

Fig. 5-13 shows the space convergence study for the sensitivity s_δ for C-N scheme with very small time step (Δt =10^{-4}). For larger Δx, we observe there exists oscillation behavior with time; For smaller Δx, 2nd order convergence speed is apparent. Fig. 5-14 shows the time convergence study for the sensitivity s_δ for C-N scheme with small spatial step (Δx =1/32). 2nd order convergence speed is achieved until Δt becomes too small when the spatial error begins to dominate. Fig. 5-15 shows the time convergence study for the sensitivity s_δ for the 1st order backward Euler scheme with a small spatial step (Δx =1/32). It is very clear that the 1st order convergence speed is obtained.

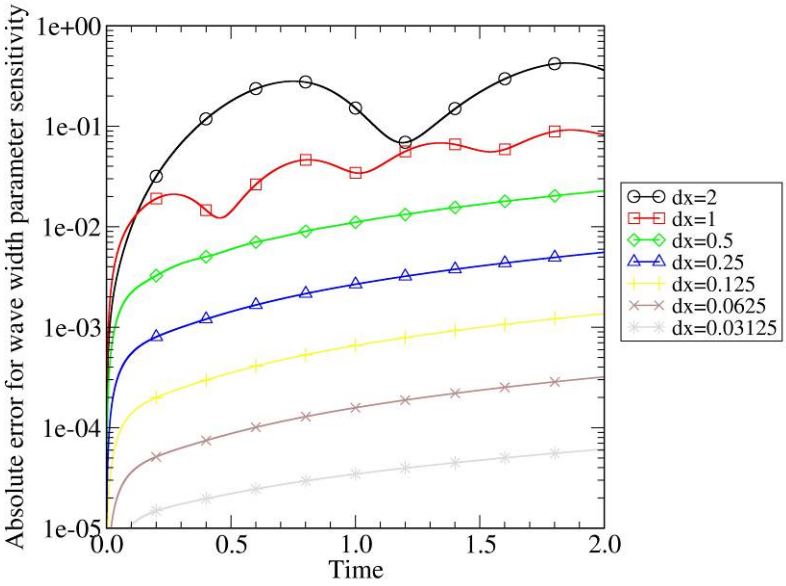

Figure 5-13: Space convergence study for the sensitivity s_δ in the thermal wave problem, C-N scheme, $\Delta t = 10^{-4}$.

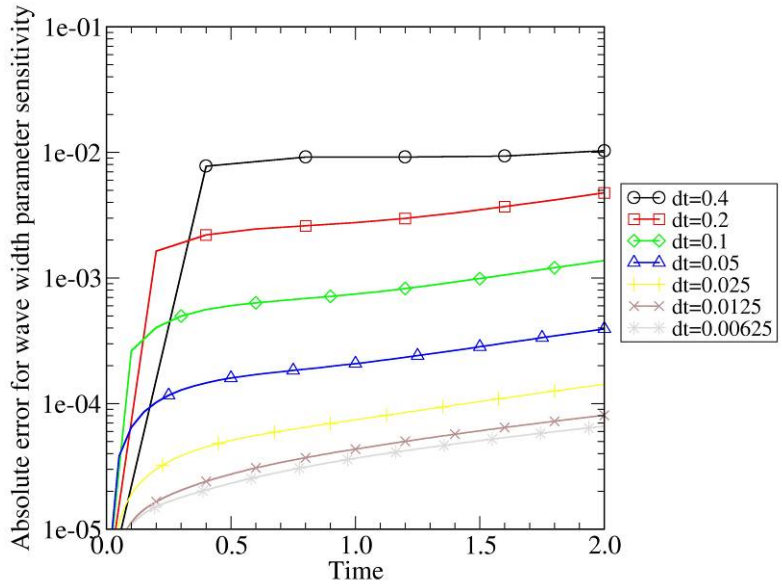

Figure 5-14: Time convergence study for the sensitivity s_δ in the thermal wave problem, C-N scheme, $\Delta x = 1/32$.

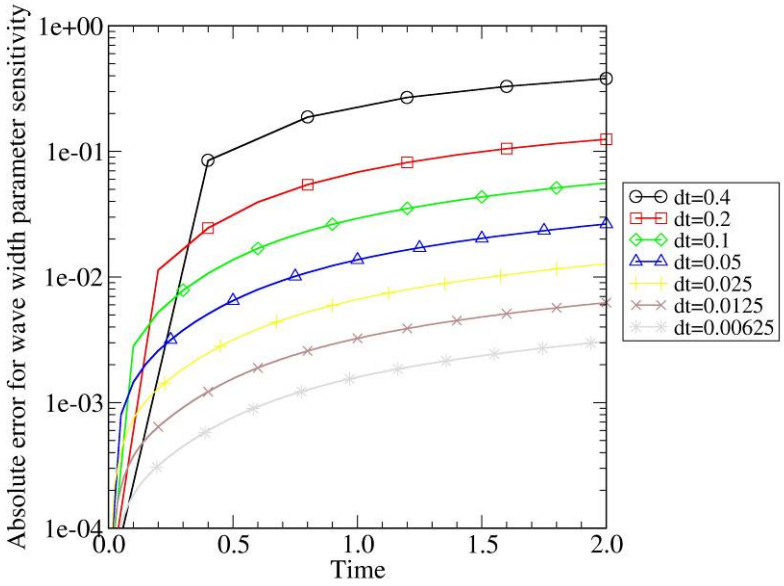

Figure 5-15: Time convergence study for the sensitivity s_δ in the thermal wave problem, backward Euler scheme, Δx =1/32.

5.3.3 Time Step Sensitivity Convergence Study and Results

The time step sensitivity analysis is different from the normal parameters as discussed in previous sections. The first question is what proper initial condition we should use for $s_{\Delta t}$. One can argue that 0 initial condition should be used since the physical problem initial condition does not depend on Δt. But one can also derive the initial condition according to $s_{\Delta t}$ analytical solution (Eq. 5-23) by setting time equals 0, same as the treatment for other normal parameter sensitivities. We'll compare the effects due to different initial conditions shortly.

Another potential error source is the treatment in Eq. 5-47. Note that the approximation is actually for time step (n-1) instead for time step n, which requires solutions at time step (n+2). To demonstrate this 1st order approximation effect, we can use the analytical solution for this term as shown below:

$$\left(\frac{\partial F}{\partial \Delta t}\right)_i = \left(\frac{1}{2}\frac{\partial^2 T}{\partial t^2}\right)_i = -\frac{1}{2}\frac{c^2}{\delta^2}\tanh\left(\frac{x-ct}{\delta}\right)\left(\left(\tanh\left(\frac{x-ct}{\delta}\right)\right)^2 - 1\right)_i . \tag{5-49}$$

Figs. 5-16 and 5-17 show the initial condition effect on the time step sensitivity $s_{\Delta t}$ for two different time steps, with analytical treatment on $\frac{\partial F}{\partial \Delta t}$. Both figures show that using the analytical initial condition for $s_{\Delta t}$ gives results much more close to the analytical

solution than with the zero initial condition. However, for large complex nonlinear PDE systems, the analytical initial condition for $s_{\Delta t}$ is usually not available. From Fig. 5-17 we notice that the numerical solution with analytical initial condition almost converges exactly to the analytical solution when a small time step is used.

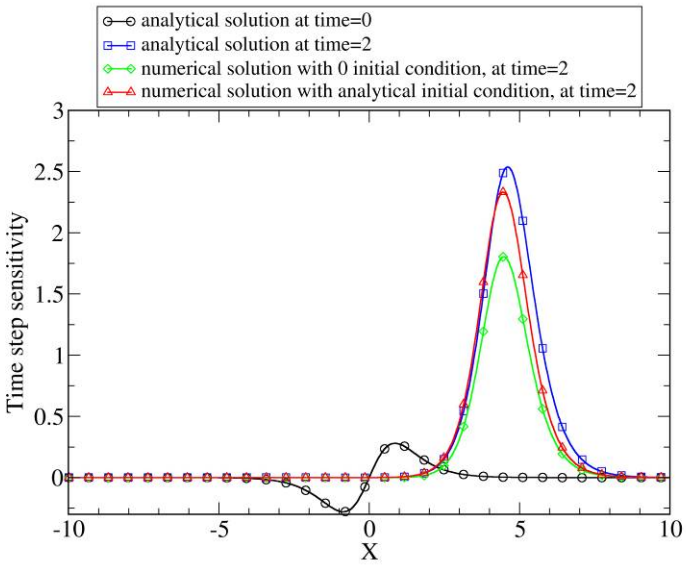

Figure 5-16: Initial condition effect on the time step sensitivity $s_{\Delta t}$ in the thermal wave problem, analytical treatment of $\frac{\partial F}{\partial \Delta t}$, backward Euler scheme, Δt =0.1, Δx =1/32.

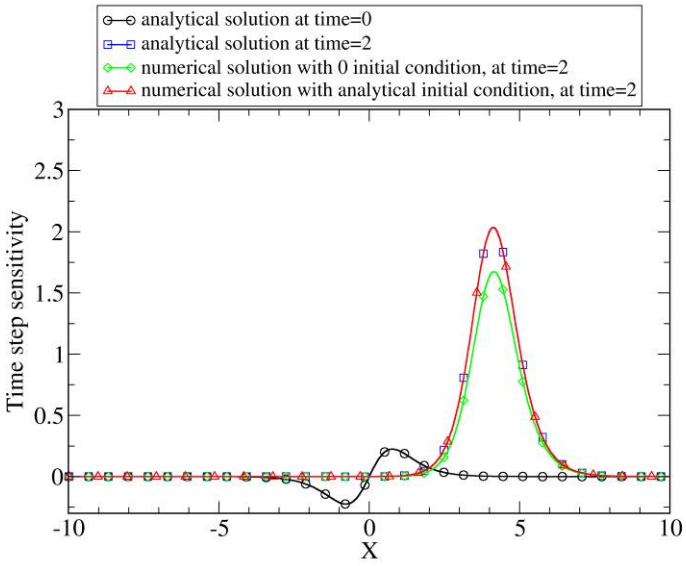

Figure 5-17: Initial condition effect on the time step sensitivity $s_{\Delta t}$ in the thermal wave problem, analytical treatment of $\frac{\partial F}{\partial \Delta t}$, backward Euler scheme, Δt =0.001, Δx =1/32.

Fig. 5-18 shows the spatial step convergence study result for $s_{\Delta t}$. A small time step was used to minimize the time step error. For larger Δx, there exists numerical oscillation with time. For smaller Δx, the $s_{\Delta t}$ errors for different Δx show 2nd order convergence speed until the time step error saturates. Fig. 5-19 shows the time step convergence study. The convergence trend is at least first order. By comparing Figs. 5-18 and 5-19 with Figs. 5-10 to 5-15, time step sensitivity analyses show very similar convergence behavior as normal physical parameter sensitivities.

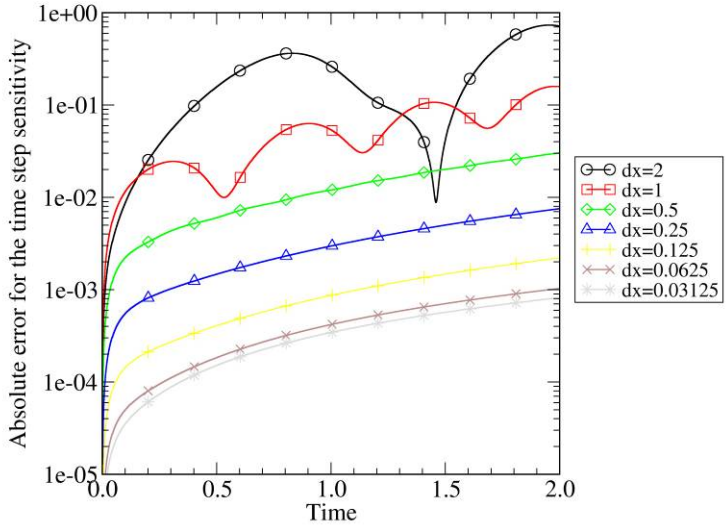

Figure 5-18: Space convergence study for the sensitivity $s_{\Delta t}$ in the thermal wave problem, analytical treatment of $\frac{\partial F}{\partial \Delta t}$, backward Euler scheme, Δt =0.001.

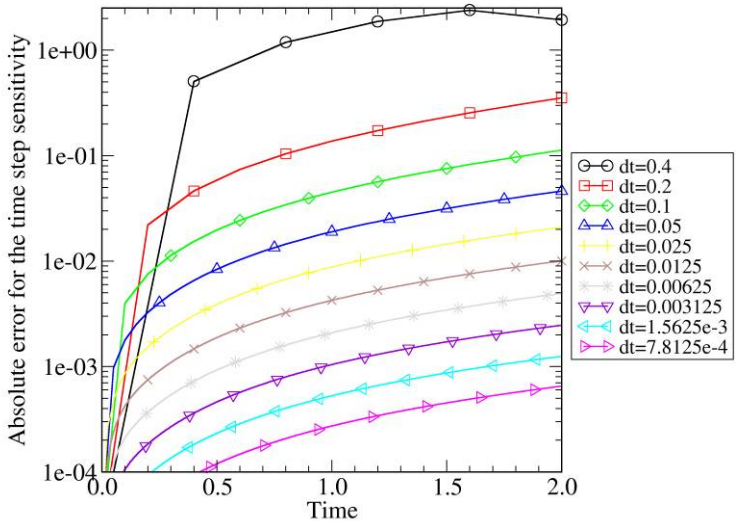

Figure 5-19: Time convergence study for the sensitivity $s_{\Delta t}$ in the thermal wave problem, analytical treatment of $\frac{\partial F}{\partial \Delta t}$, backward Euler scheme, Δx =1/32.

Consider the effect of approximate treatment on $\frac{\partial F}{\partial \Delta t}$ according to Eq. 5-47. For time iteration 1, the solution at time iteration (-1) is calculated by using the analytical solution. In the cases without analytical solutions, the time step sensitivity iteration can start from the 2nd time step so that the numerical solution at time step iteration 1 will be available to calculate $\frac{\partial F}{\partial \Delta t}$ numerically. Figs. 5-20 and 5-21 show the initial condition effect on the time step sensitivity $s_{\Delta t}$ for two different time steps. Both figures show that using the analytical initial condition for $s_{\Delta t}$ gives results more close to the analytical solution than with the zero initial condition. Therefore, accurate initial condition for $s_{\Delta t}$ is important to calculate $s_{\Delta t}$. From the small time step figure we note that the numerical solution can converge to the analytical solution. Therefore, numerical treatment on $\frac{\partial F}{\partial \Delta t}$ according to Eq. 5-47 will not cause large error in the solution of $s_{\Delta t}$.

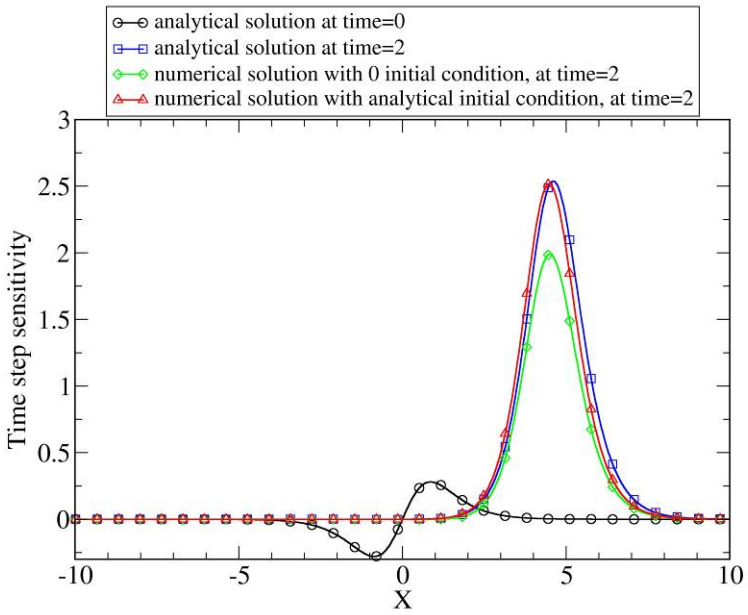

Figure 5-20: Initial condition effect on the time step sensitivity $s_{\Delta t}$ in the thermal wave problem, approximate treatment on $\frac{\partial F}{\partial \Delta t}$, backward Euler scheme, Δt =0.1, Δx =1/32.

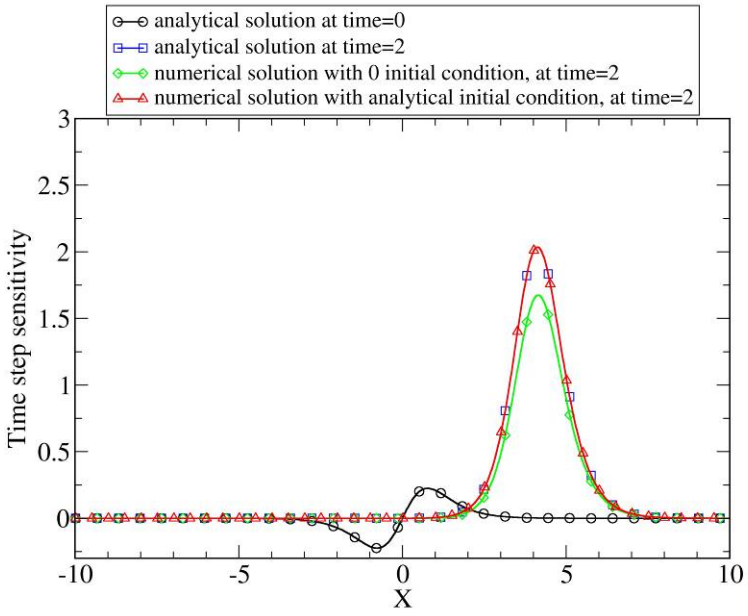

Figure 5-21: Initial condition effect on the time step sensitivity $s_{\Delta t}$ in the thermal wave problem, approximate treatment on $\frac{\partial F}{\partial \Delta t}$, backward Euler scheme, Δt =0.001, Δx =1/32.

Fig. 5-22 shows the spatial step convergence study result for $s_{\Delta t}$. A small time step was used to minimize time step error. For larger Δx, there exists numerical oscillation with time. For smaller Δx, the $s_{\Delta t}$ errors for different Δx converge with 2nd order speed until

other errors saturate. Fig. 5-23 shows the time step convergence study. The convergence trend is at least first order for all the time steps.

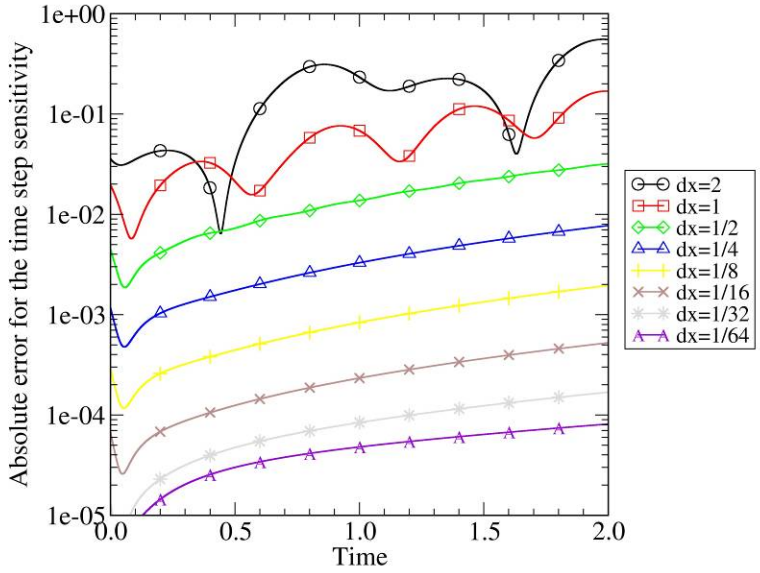

Figure 5-22: Space convergence study for the sensitivity $s_{\Delta t}$ in the thermal wave problem, approximate treatment on $\frac{\partial F}{\partial \Delta t}$, backward Euler scheme, Δt =0.0001.

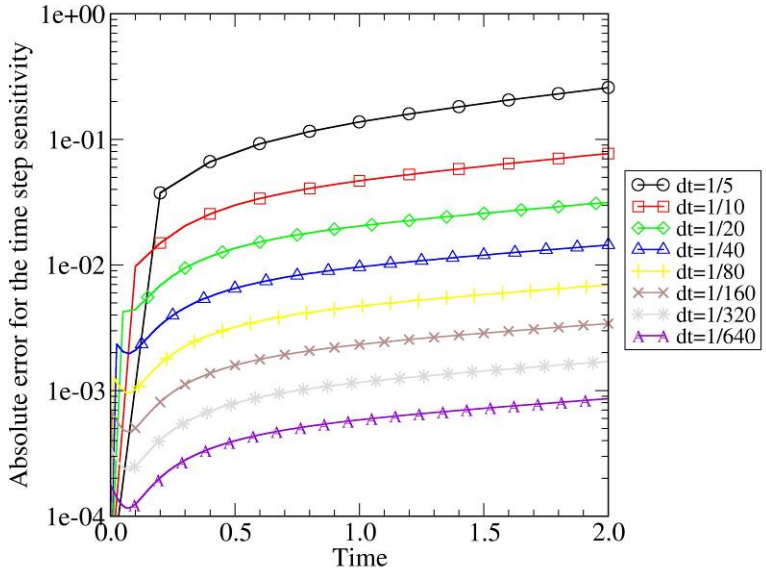

Figure 5-23: Time convergence study for the sensitivity $s_{\Delta t}$ in the thermal wave problem, approximate treatment on $\frac{\partial F}{\partial \Delta t}$, backward Euler scheme, Δx =1/64.

Fig. 5-24 shows an example how to interpret $s_{\Delta t}$ and how to use it. In this figure, the solid diamond line is the thermal wave problem analytical solution at time equal to 2. The cross line is the numerical result with a time step of 0.1, which is the reference time step. The circle line is the direct numerical result with the reference time step reduced by 99% and the square line is the direct numerical result with the reference time step increased by 99%. We can take these three lines as the time step convergence study with time steps reduced from 0.199 to 0.1, and further to a very small value 0.001. We can see the smallest time step generates a solution almost exactly same as the analytical solution. The two triangle lines are calculated with Eq. 2-19 according to the numerical solution with the reference Δt and its corresponding $s_{\Delta t}$. So these two lines form a range, where the exact solution should and actually does fall in. Because in the converged range larger Δt always generate a solution with more errors, the error bars actually can be reduced by almost half – between the cross reference solution line and the down triangle line.

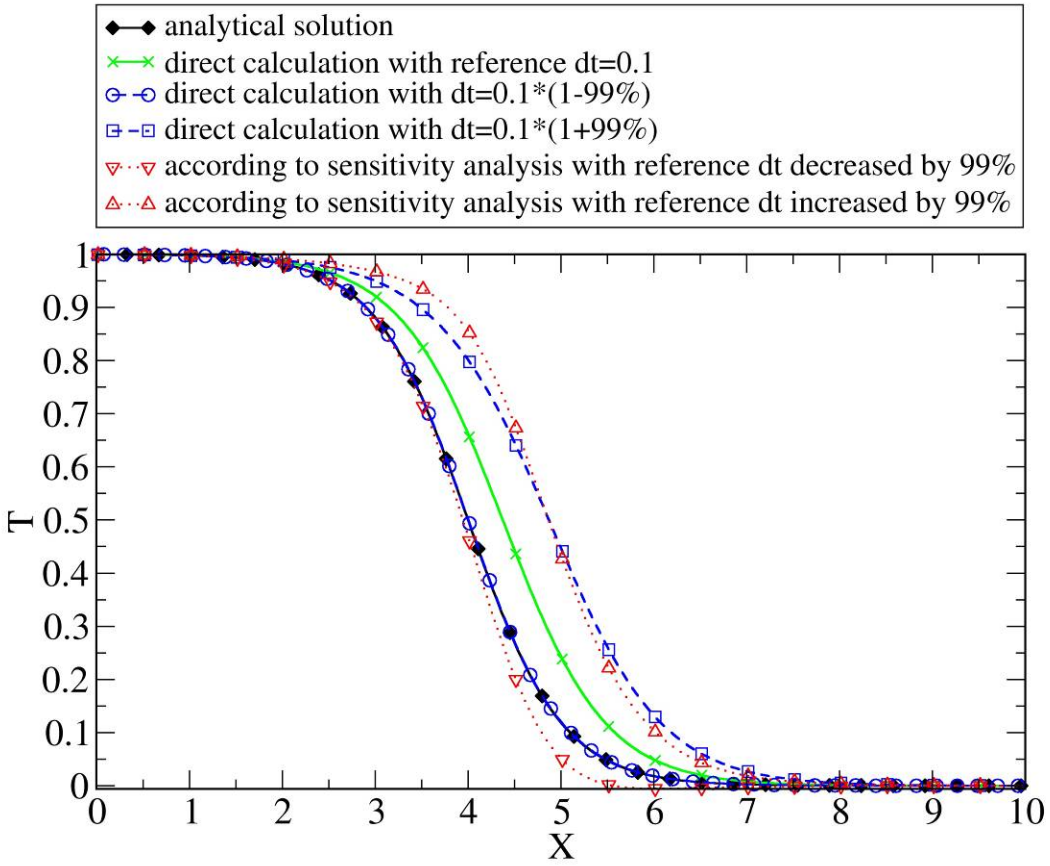

Figure 5-24: Comparison of analytical solution, direct time convergence study, and numerical error bars from sensitivity analysis result for the thermal wave problem, backward Euler scheme, Δx =0.03125, time at 2.

5.3.4 Sensitivity Comparison

When all the parameter sensitivity solutions are available, a systematic comparison of parameter sensitivities can be performed. Eq. (2-19) can be rewritten as

$$\mathbf{Y}_{\pm} = \mathbf{Y} \pm \mathbf{s}_p \frac{\Delta p}{p} p, \tag{5-50}$$

where $\mathbf{s}_p$ is the sensitivity solution, p the reference value for the parameter, and $\frac{\Delta p}{p}$ the uncertainty range given by the physical models, which can be provided by experts in those physical models or determined by accuracy requirement. We are only interested in the parameters where the multiplication of three variables is large. To reduce uncertainty from one parameter, people can either improve the measurement on the parameter to reduce $\frac{\Delta p}{p}$ or propose better models to reduce s_p.

Fig. 5-25 compares sensitivity $s_{\Delta t}$, s_c, and s_δ at t=0.1 and t=2. The solid lines are for time at 0.1 and the dash lines are for time at 2. Lines with circle symbols are $s_{\Delta t}$; lines with square symbols are s_c; and lines with diamond symbols are s_δ. The relative ranking of $s_{\Delta t}$, s_c, and s_δ varies with time and location. Near the start, the solution sensitivity with respective to the wave speed s_c is smaller than the solution sensitivity with respective to the wave width s_δ and the solution sensitivity with respective to the time step $s_{\Delta t}$. At later time, s_c outgrows s_δ. Also we can notice that $s_{\Delta t}$ is larger than s_c and s_δ in most locations for most time. However, we cannot say the solution is sensitive to the time step since the time step is very small so that $\mathbf{s}_{\Delta t} \frac{\delta(\Delta t)}{\Delta t} \Delta t$ is also small.

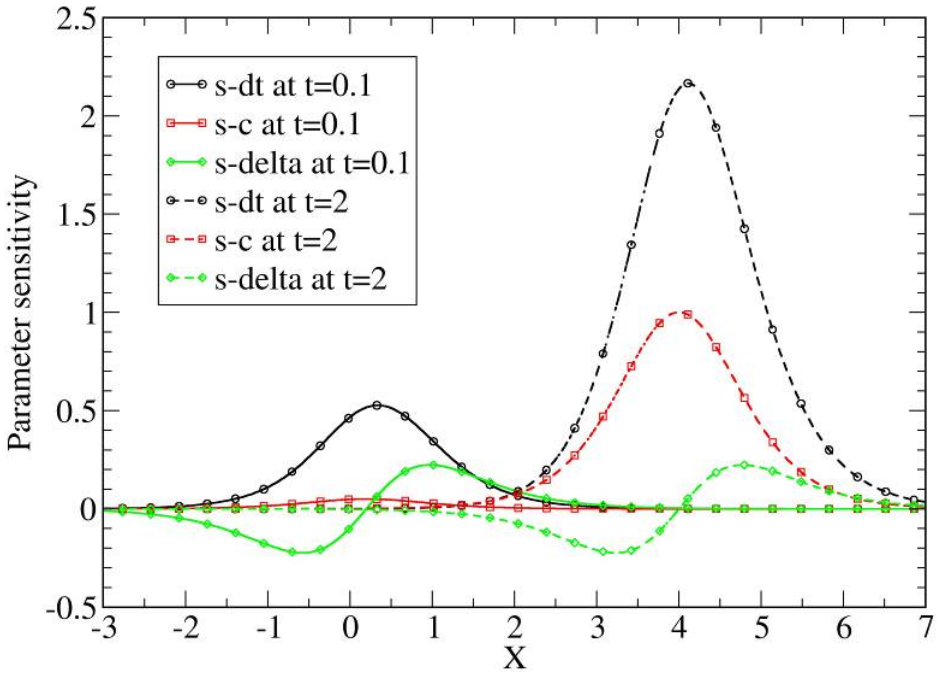

Figure 5-25: Comparison of sensitivities $s_{\Delta t}$, s_c, and s_δ at t=0.1 and t=2 in the thermal wave problem, backward Euler scheme, Δx =0.03125, Δt =0.001.

Fig. 5-26 compares the sensitivity analysis results from the forward sensitivity analysis method (shown as dash lines) and from direct calculations (shown as discrete points) by changing the wave speed c by ±10%. The forward sensitivity results match the direct calculation results very well. Note that the forward sensitivity only requires one run while the direct calculations require three runs. When we reduce the uncertainty range for c to ±5%, the forward sensitivity results match the direct calculation results even much better, as shown in Fig. 5-27.

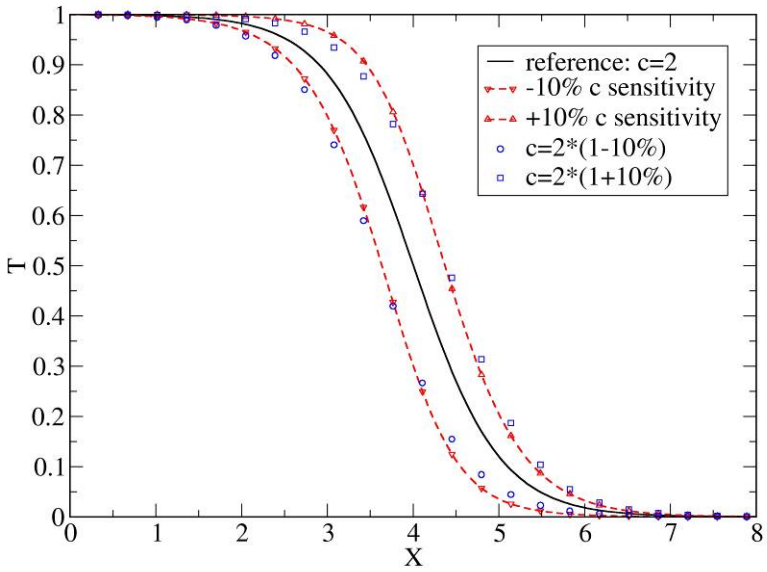

Figure 5-26: Comparison of sensitivity analyses for the wave speed parameter between forward sensitivity analysis and direct calculation in the thermal wave problem, t=2, backward Euler scheme, Δx =0.03125, Δt =0.001, uncertainty range: ±10%.

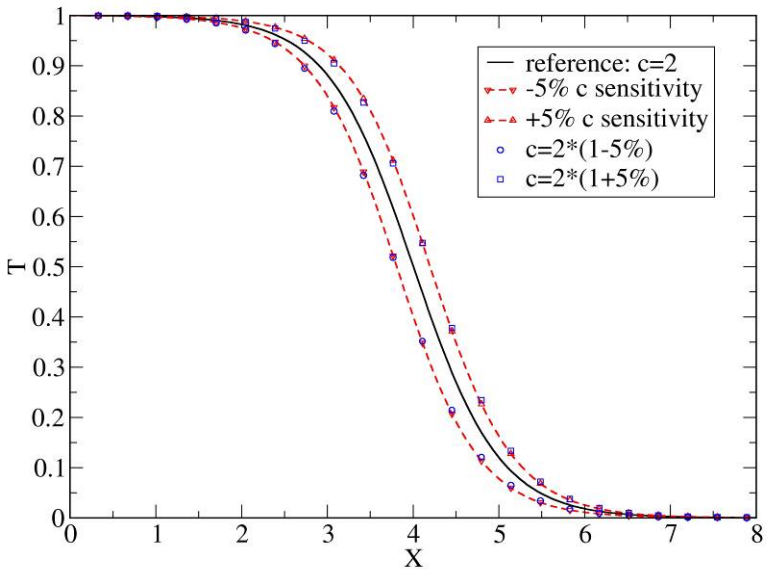

Figure 5-27: Comparison of sensitivity analyses for the wave speed parameter between forward sensitivity analysis and direct calculation in the thermal wave problem, t=2, backward Euler scheme, Δx =0.03125, Δt =0.001, uncertainty range: ±5%.

Fig. 5-28 compares the sensitivity analysis results from the forward sensitivity analysis method (shown as dash lines) and from direct calculations (shown as discrete points) by changing the wave width δ by ±10%. The forward sensitivity results match the direct calculation results excellently. Therefore, we can reliably use the forward sensitivity to evaluate the parameter uncertainty effect on solution.

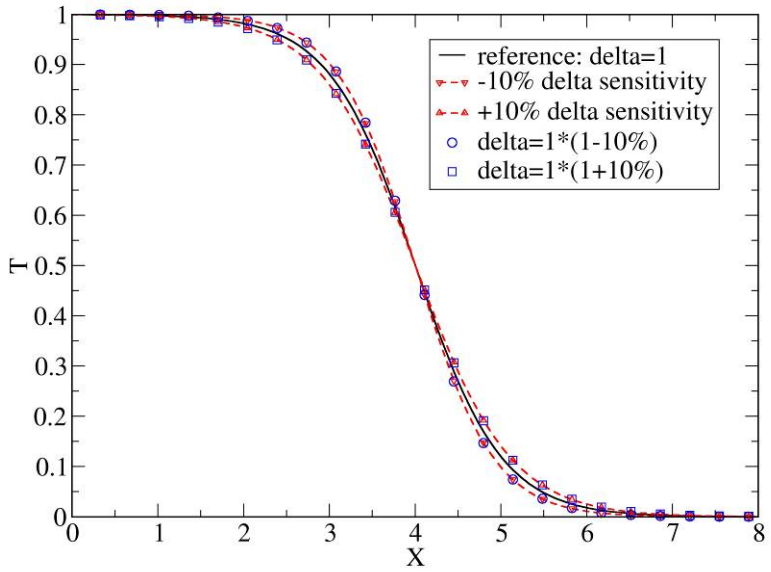

Figure 5-28: Comparison of sensitivity analyses for the wave width parameter between forward sensitivity analysis and direct calculation in the thermal wave problem, t=2, backward Euler scheme, Δx =0.03125, Δt =0.001, uncertainty range: ±10%.

The forward sensitivity analysis provides a systematic method to evaluate the parameter sensitivity effects on solution, along with time and space convergence information. Fig. 5-29 compares sensitivity effects from time step, wave speed, and wave width parameters for a large time step (0.1) and a very small spatial step (1/32). We can readily notice that the solution is still very sensitive to the time step, which means the solution is not well converged. The uncertainty bar from the time step is much larger than the uncertainty bar from the wave width parameter and is at the same order with the uncertainty bar from the wave speed parameter. Therefore, the solution along with the sensitivity analysis is not reliable. One should use a smaller time step in order to obtain accurate solution and sensitivity analysis results. Fig. 5-30 shows the similar results for a very small time step (0.001) and a very small spatial step (1/32). In this case, the solution is not sensitive to the time step, therefore the solution and sensitivity results are reliable. These comparisons just show how important to consider time and space convergences when performing uncertainty analysis. In conventional Monte Carlo type of uncertainty analysis, people tend to use large time steps and coarse grids in order to do large amount of calculations without considering numerical errors. The sensitivity results from such practices often contain large error and even are totally wrong. Including the time step and space step as special sensitivity parameters provides a new method to avoid such pitfalls and improves both accuracy and efficiency.

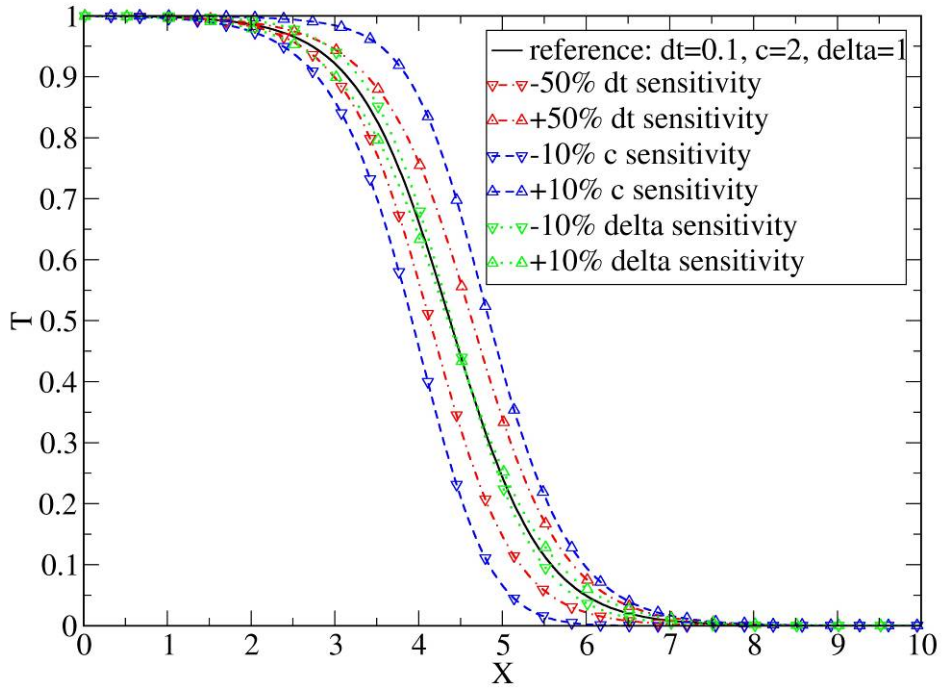

Figure 5-29: Comparison of sensitivity effects from time step, wave speed, and wave width for the thermal wave problem, t=2, backward Euler scheme, Δx =0.03125, Δt =0.1.

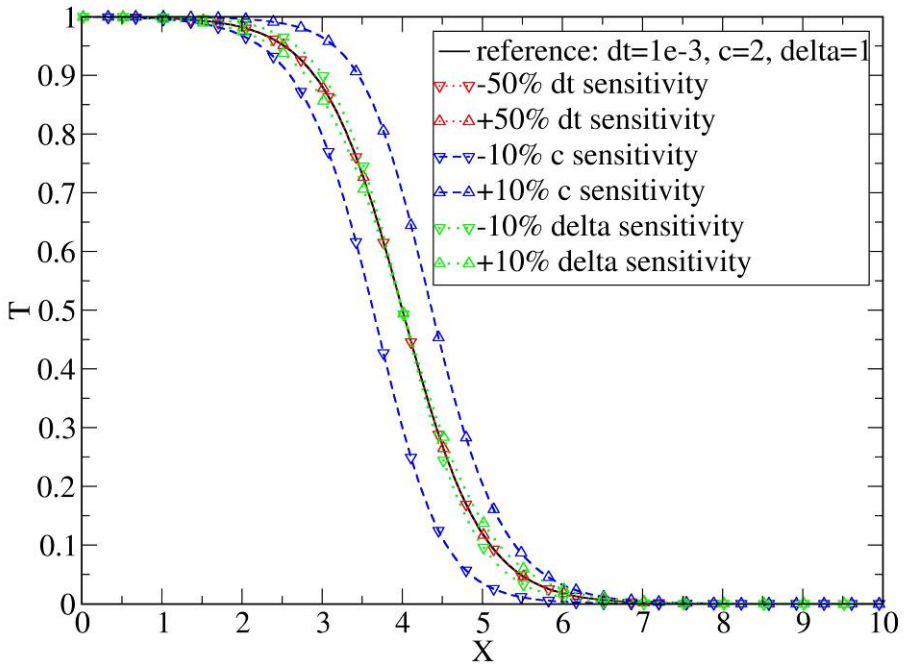

Figure 5-30: Comparison of sensitivity effects from time step, wave speed, and wave width for the thermal wave problem, t=2, backward Euler scheme, Δx =0.03125, Δt =0.001.

6. NONLINEAR DIFFUSION PROBLEM

6.1 Physical Model

We will use a nonlinear diffusion problem as another example to investigate the forward sensitivity method. The following is the equation:

$$\frac{\partial T(x,t,\alpha)}{\partial t} - \frac{\partial}{\partial x}\left(T(x,t,\alpha)^{\alpha} \frac{\partial}{\partial x} T(x,t,\alpha) \right) = mms(x,t,\alpha), \tag{6-1}$$

for $x \in [0,1]$, and $t \geq 0$. In Eq. 6-1 α is a constant parameter which does not change with time, $mms(x,t,\alpha)$ the source term for the manufactured solution depending on the assumed analytical solution, which can be calculated by substituting an assumed solution $T(x,t,\alpha)$ into the LHS. With the analytical solution available, the numerical errors can be accurately measured. The above problem meets the following boundary conditions:

$$T(0,t,\alpha) = a, \tag{6-2}$$

$$T(1,t,\alpha) = b, \tag{6-3}$$

where a=1, and b=0.1. The initial condition can be obtained from the constructed analytical solution which should be a smooth function with time, space, and the nonlinearity index α. For example, we can assume the following analytical solution:

$$T(x,t,\alpha) = 1 - 0.9x^{\alpha \cdot t+1}, \tag{6-4}$$

The initial condition then is:

$$T(x,0,\alpha) = 1 - 0.9x, \tag{6-5}$$

Substitute Eq. 6-4 into the LHS of Eq. 6-1, we obtain:

$$\begin{aligned} mms(x,t,\alpha) = & -0.9\alpha \cdot x^{\alpha \cdot t+1} \cdot \ln x - 0.81\alpha \cdot \left(1 - 0.9x^{\alpha \cdot t+1}\right)^{\alpha-1} \cdot x^{2\alpha \cdot t} \cdot (\alpha \cdot t+1)^2 \\ & + 0.9\alpha \cdot \left(1 - 0.9x^{\alpha \cdot t+1}\right)^{\alpha} \cdot x^{\alpha \cdot t-1} \cdot t \cdot (\alpha \cdot t+1) \end{aligned} \tag{6-6}$$

This test problem provides the flexibility to adjust the nonlinearity and observe the sensitivity of the solution with the nonlinearity index α:

$$s_{\alpha} = \frac{dT}{d\alpha}. \tag{6-7}$$

s_{α} can be directly calculated by substituting Eq. 6-4 into Eq. 6-7,

$$s_{\alpha}(x,t,\alpha) = -0.9x^{\alpha \cdot t+1} \cdot t \cdot \ln x, \tag{6-8}$$

Figs. 6-1 to 6-6 show the analytical solution (Eq. 6-5), the source term for the manufactured solution (Eq. 6-6), and the analytical sensitivity solution for α, respectively, for both cases of $\alpha = 0.7$ and $\alpha = 7$. For small α, we call the problem a weak nonlinear diffusion problem; and for large α, i.e., α=7, we call it a strong nonlinear diffusion problem. From Figs. 6-1 and 6-2, we notice that the nonlinearity increases with time by starting with a linear problem. This problem provides a good test covering both linear and nonlinear problems. For the same time, the strong nonlinear diffusion problem exhibits much larger gradient at the wave front than the weak nonlinear diffusion problem. From Figs. 6-3 and 6-4, we note that the source terms for weak and strong nonlinear problems show quite different behaviors. Figs. 6-5 and 6-6 show that the α sensitivity decreases by an order when α increases from 0.7 to 7. Because quite different behaviors between weak and strong nonlinear diffusion problems, we'll show the sensitivity analysis results separately for both cases.

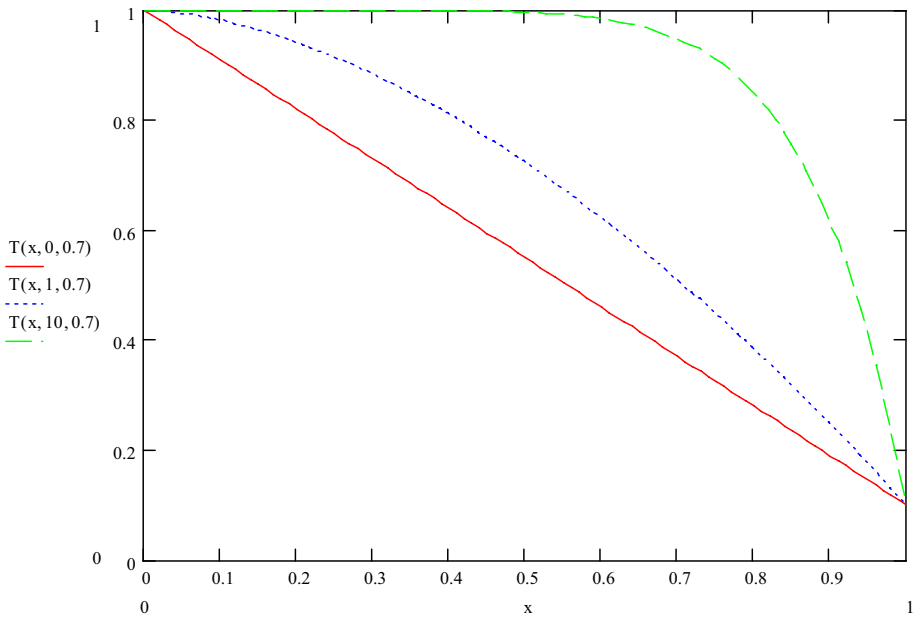

Figure 6-1: Weak nonlinear diffusion problem analytical solution as function of time.

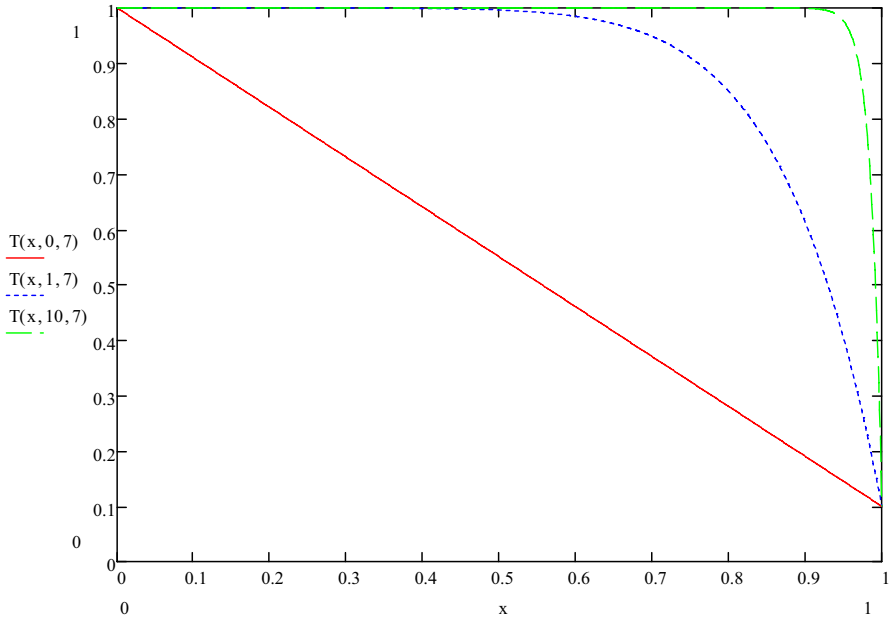

Figure 6-2: Strong nonlinear diffusion problem analytical solution as function of time.

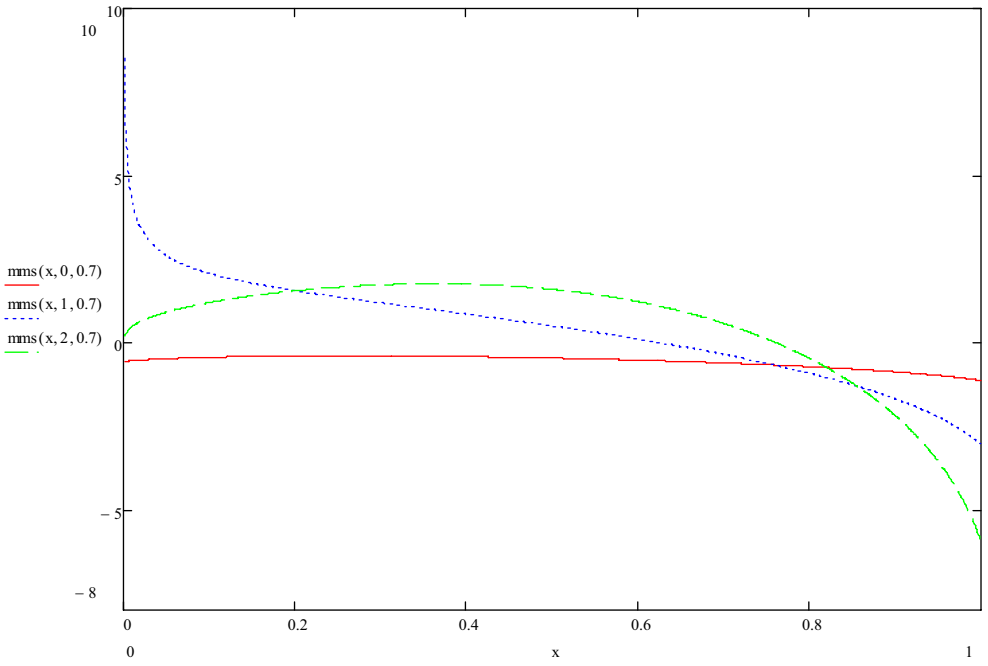

Figure 6-3: Source term for the manufactured solution in the weak nonlinear diffusion problem.

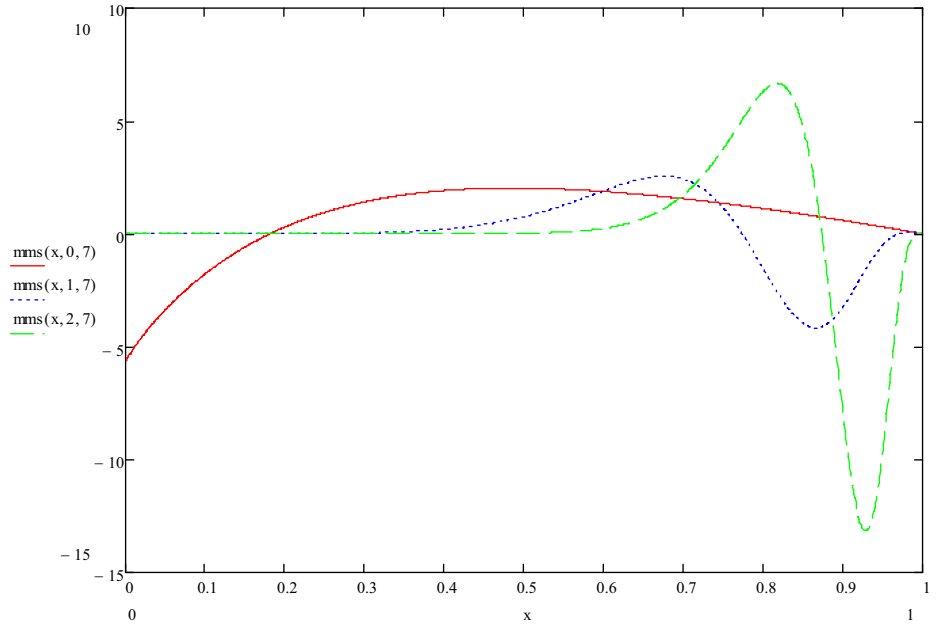

Figure 6-4: Source term for the manufactured solution in the strong nonlinear diffusion problem.

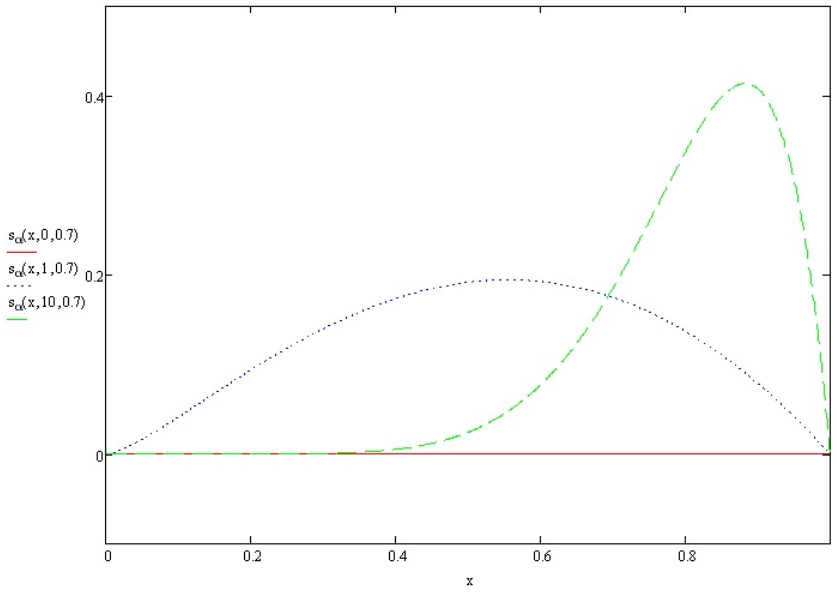

Figure 6-5: Analytical solution for the sensitivity s_α in the weak nonlinear diffusion problem.

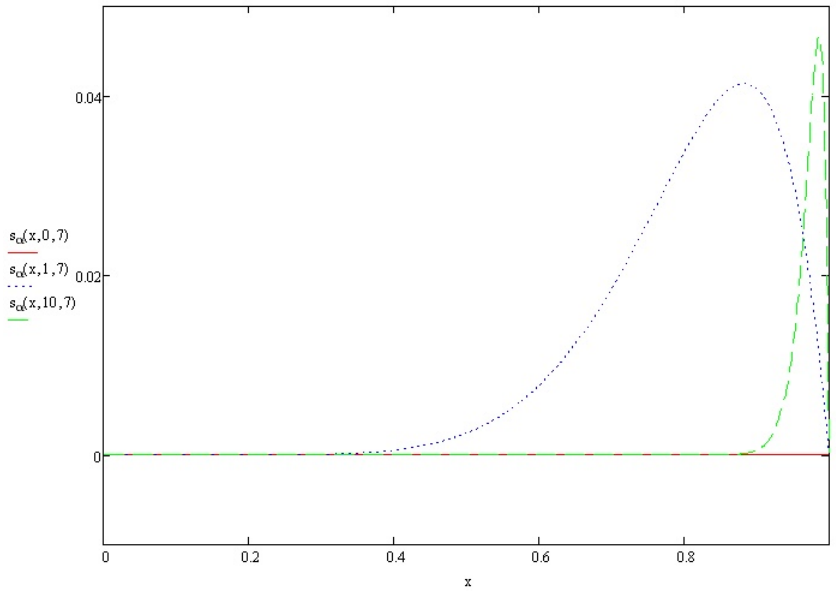

Figure 6-6: Analytical solution for the sensitivity s_α in the strong nonlinear diffusion problem.

According to Eqs 4-1 and 4-4, the time scale and length scale for the nonlinear diffusion problem can be derived as:

$$\tau_T(x,t,\alpha) = \frac{x^{\alpha\cdot t+1} - \frac{10}{9}}{\alpha \cdot x^{\alpha\cdot t+1} \cdot \ln x}, \tag{6-9}$$

$$L_T(x,t,\alpha) = \left| \frac{x^{\alpha\cdot t+1} - \frac{10}{9}}{x^{\alpha\cdot t} \cdot (\alpha\cdot t+1)} \right|. \tag{6-10}$$

Figs. 6-7 and 6-8 show the time scales for the weak and strong nonlinear diffusion problems at three times. The time scale quickly increases with time. We are only interested in the minimum time scales, which can be numerically solved according to Eq. 6-9. The minimum time scale at time 0 for the weak nonlinear diffusion problem is about 2.3; and the minimum time scale at time 0 for the strong nonlinear diffusion problem is about 0.23. Fig 6-9 shows the length scale for the weak nonlinear diffusion problem at three times. From this figure and Eq. 6-10, we note that the minimum length scales always appear at the right side boundary:

$$L_{T\min}(t,\alpha) = \frac{1}{9(\alpha\cdot t+1)}. \tag{6-11}$$

Figs. 6-10 and 6-11 show the minimum length scales as a function of time for the weak and strong nonlinear diffusion problems, respectively. The minimum length scales decrease with time. At time equal 0, both minimum length scales are about 0.1. However,

the minimum length scale for the strong nonlinear diffusion problem drops much faster than the minimum length scale for the weak nonlinear diffusion problem.

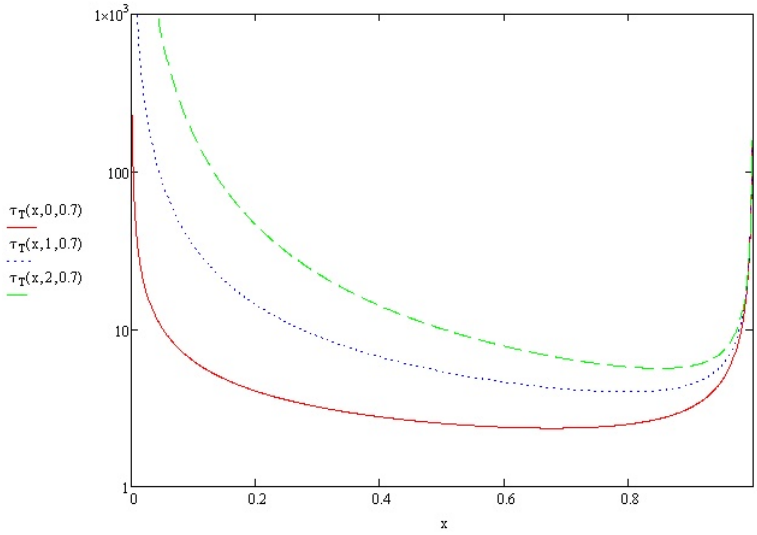

Figure 6-7: Time scales for the weak nonlinear diffusion problem at three times: 0, 1, and 2.

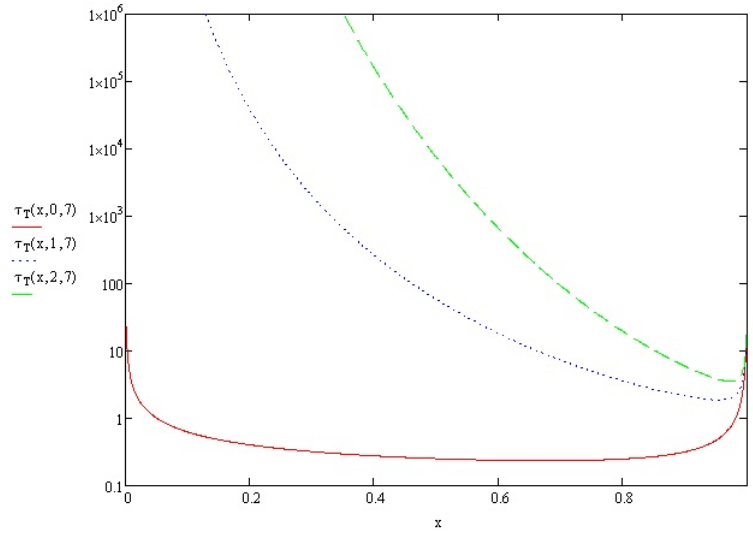

Figure 6-8: Time scales for the strong nonlinear diffusion problem at three times: 0, 1, and 2.

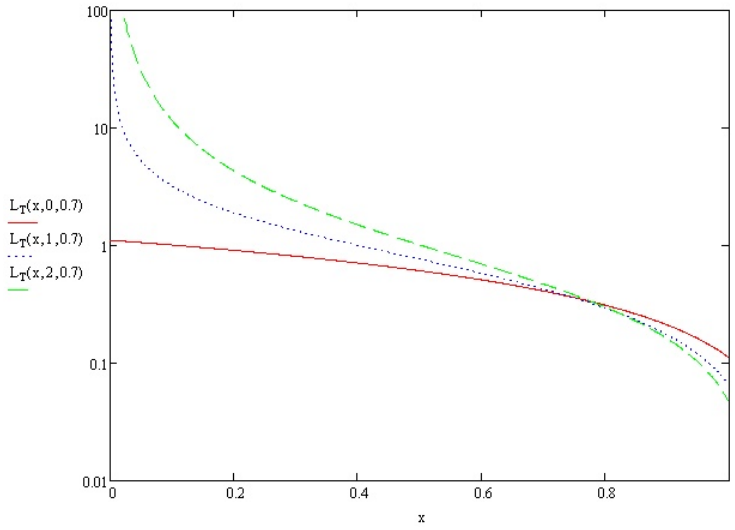

Figure 6-9: Length scales for the weak nonlinear diffusion problem at three times: 0, 1, and 2.

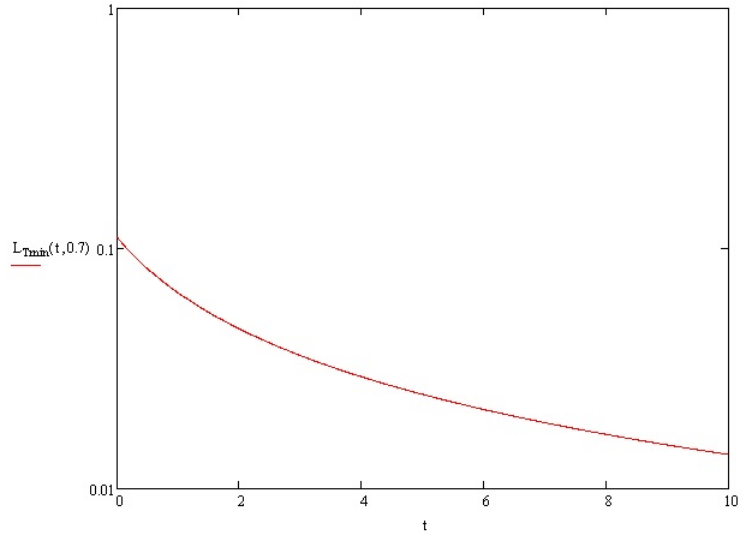

Figure 6-10: The minimum length scale as a function of time for the weak nonlinear diffusion problem.

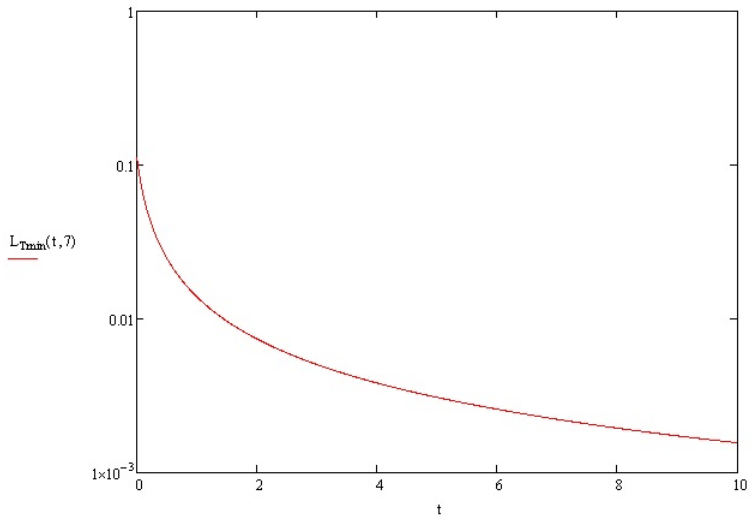

Figure 6-11: The minimum length scale as a function of time for the strong nonlinear diffusion problem.

According to Eqs 4-1, 4-4, and 6-8, the time scale and length scale for s_α can be derived as:

$$\tau_{s_\alpha}(x,t,\alpha) = \left| \frac{t}{\alpha \cdot t \cdot \ln x + 1} \right|, \tag{6-12}$$

$$L_{s_\alpha}(x,t,\alpha) = \left| \frac{x}{1 + \alpha \cdot t + \frac{1}{\ln x}} \right|. \tag{6-13}$$

Figs. 6-12 and 6-13 show the time scales of s_α for the weak and strong nonlinear diffusion problems at three times, respectively. The time scale is 0 for time equal 0 since $s_\alpha = 0$. The minimum time scale always appears at x=0 and equals to 0. Figs 6-14 and 6-15 show the length scales of s_α for the weak and strong nonlinear diffusion problems at three times, respectively. From these figures and Eq. 6-13, we note that the minimum length scales always appear at the left and right side boundaries and equal to 0.

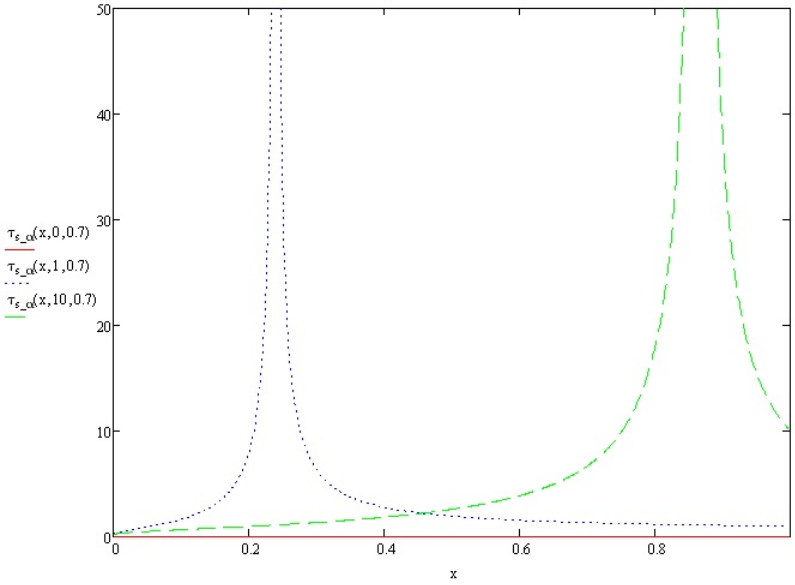

Figure 6-12: Time scales of s_α for the weak nonlinear diffusion problem at three times: 0, 1, and 2.

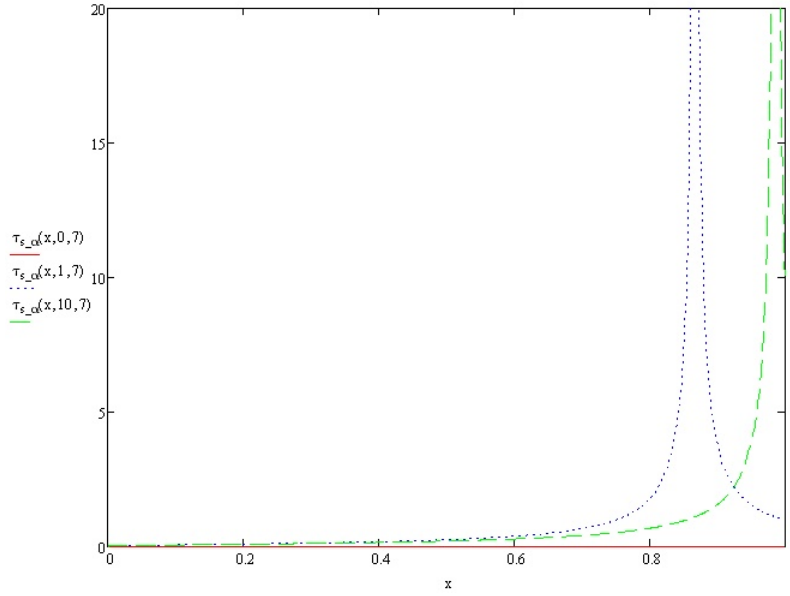

Figure 6-13: Time scales of s_α for the strong nonlinear diffusion problem at three times: 0, 1, and 2.

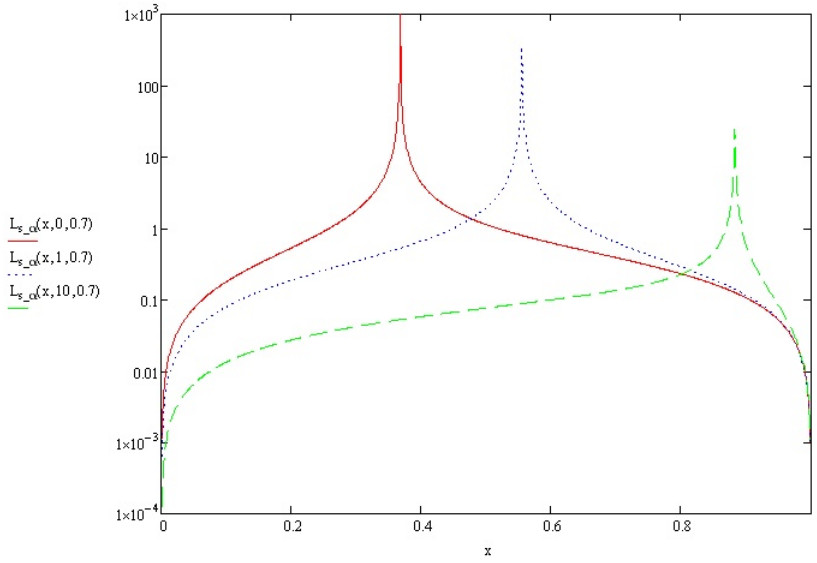

Figure 6-14: Length scales of s_α for the weak nonlinear diffusion problem at three times: 0, 1, and 2.

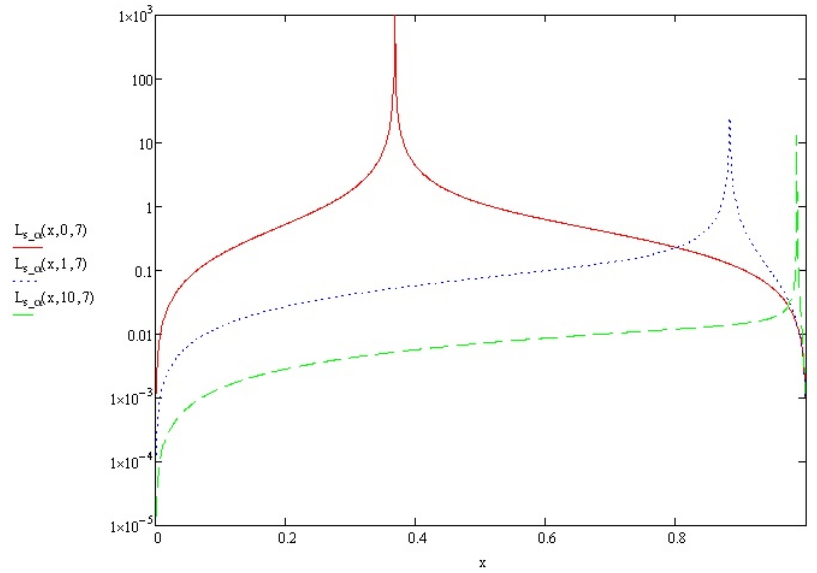

Figure 6-15: Length scales of s_α for the strong nonlinear diffusion problem at three times: 0, 1, and 2.

6.2 Numerical Models

We use Newton's method to solve the physical problem defined by Eq. 6-1, 6-2, 6-3, and 6-5 and the associated sensitivity problem. F function in Eq. 6-1 for the physical problem and associated sensitivity problem as described by Eq. 2-7 and 2-8 is,

$$F(x,t,T,\alpha)=\frac{\partial}{\partial x}\left(T^{\alpha}\frac{\partial T}{\partial x}\right)+mms(x,t,\alpha). \tag{6-14}$$

The discretized nonlinear residual equation for the physical problem at time step n+1 and control volume i is same as Eq. (5-28):

$$res_i(\mathbf{T}^{n+1})=\frac{T_i^{n+1}-T_i^n}{\Delta t}-\theta\cdot F^{n+1}-(1-\theta)\cdot F^n, \tag{5-28}$$

The diffusion term can be discretized with center difference method:

$$\frac{\partial}{\partial x}\left(T^{\alpha}\frac{\partial T}{\partial x}\right)_i=\frac{1}{\Delta x^2}\left(\left(\frac{T_i+T_{i+1}}{2}\right)^{\alpha}(T_{i+1}-T_i)-\left(\frac{T_{i-1}+T_i}{2}\right)^{\alpha}(T_i-T_{i-1})\right), \tag{6-15}$$

$$for \quad i=2,...,I-1$$

where subscript i represents the spatial control volume index, ranging from 2 to I-1. Note that the solution value is located at the center of each control volume. For the first type of boundary conditions defined by Eqs 6-2 and 6-3, the boundary values (i=0 or i=I+1) are located at the boundary of the control volume. Therefore Eq. (6-15) needs to be adjusted to reflect the half control volume fact:

$$\frac{\partial}{\partial x}\left(T^{\alpha}\frac{\partial T}{\partial x}\right)_1=\frac{1}{\Delta x^2}\left(\left(\frac{T_1+T_2}{2}\right)^{\alpha}(T_2-T_1)-2\cdot T_0{}^{\alpha}(T_1-T_0)\right), \tag{6-16}$$

$$\frac{\partial}{\partial x}\left(T^{\alpha}\frac{\partial T}{\partial x}\right)_I=\frac{1}{\Delta x^2}\left(2\cdot T_{I+1}{}^{\alpha}(T_{I+1}-T_I)-\left(\frac{T_{I-1}+T_I}{2}\right)^{\alpha}(T_I-T_{I-1})\right), \tag{6-17}$$

Two different methods are used to form the problem residue Jacobian matrix defined by Eq. 3-3. The first one uses direct evaluation method as defined by Eq. 3-3 and the second one uses approximate method defined by Eq. 3-4. Note that the Jacobian matrix is tridiagonal in this 1-D problem:

$$\widetilde{\mathbf{J}}=tridiag(\widetilde{J}_{i,i-1},\widetilde{J}_{i,i},\widetilde{J}_{i,i+1}). \tag{5-33}$$

According to Eqs. 3-3, 5-28, 6-14, 6-15, 6-16, and 6-17, direct evaluation Jacobian matrix inputs are:

$$\widetilde{J}_{i,i-1}=\frac{\partial res_i(\mathbf{T}^{n+1})}{\partial T_{i-1}^{n+1}}$$
$$=\frac{\theta}{\Delta x^2}\left[-\left(\frac{T_{i-1}^{n+1}+T_i^{n+1}}{2}\right)^{\alpha}+\frac{\alpha}{2}\left(\frac{T_{i-1}^{n+1}+T_i^{n+1}}{2}\right)^{\alpha-1}\left(T_i^{n+1}-T_{i-1}^{n+1}\right)\right], \quad (6\text{-}18)$$
$$for \quad i=2,...,I$$

$$\widetilde{J}_{i,i}=\frac{\partial res_i(\mathbf{T}^{n+1})}{\partial T_i^{n+1}}$$
$$=\frac{1}{\Delta t}+\frac{\theta}{\Delta x^2}\left[\left(\frac{T_i^{n+1}+T_{i+1}^{n+1}}{2}\right)^{\alpha}-\frac{\alpha}{2}\left(\frac{T_i^{n+1}+T_{i+1}^{n+1}}{2}\right)^{\alpha-1}\left(T_{i+1}^{n+1}-T_i^{n+1}\right)\right], \quad (6\text{-}19)$$
$$+\frac{\theta}{\Delta x^2}\left[\left(\frac{T_{i-1}^{n+1}+T_i^{n+1}}{2}\right)^{\alpha}+\frac{\alpha}{2}\left(\frac{T_{i-1}^{n+1}+T_i^{n+1}}{2}\right)^{\alpha-1}\left(T_i^{n+1}-T_{i-1}^{n+1}\right)\right]$$
$$for \quad i=2,...,I-1$$

$$\widetilde{J}_{1,1}=\frac{\partial res_1(\mathbf{T}^{n+1})}{\partial T_1^{n+1}}$$
$$=\frac{1}{\Delta t}+\frac{\theta}{\Delta x^2}\left[\left(\frac{T_1^{n+1}+T_2^{n+1}}{2}\right)^{\alpha}-\frac{\alpha}{2}\left(\frac{T_1^{n+1}+T_2^{n+1}}{2}\right)^{\alpha-1}\left(T_2^{n+1}-T_1^{n+1}\right)\right], \quad (6\text{-}20)$$
$$+\frac{\theta}{\Delta x^2}\left[2\left(T_0^{n+1}\right)^{\alpha}\right]$$

$$\widetilde{J}_{I,I}=\frac{\partial res_I(\mathbf{T}^{n+1})}{\partial T_I^{n+1}}$$
$$=\frac{1}{\Delta t}+\frac{\theta}{\Delta x^2}\left[2\cdot\left(T_{I+1}^{n+1}\right)^{\alpha}\right] \quad , \quad (6\text{-}21)$$
$$+\frac{\theta}{\Delta x^2}\left[\left(\frac{T_{I-1}^{n+1}+T_I^{n+1}}{2}\right)^{\alpha}+\frac{\alpha}{2}\left(\frac{T_{I-1}^{n+1}+T_I^{n+1}}{2}\right)^{\alpha-1}\left(T_I^{n+1}-T_{I-1}^{n+1}\right)\right]$$

$$\widetilde{J}_{i,i+1}=\frac{\partial res_i(\mathbf{T}^{n+1})}{\partial T_{i+1}^{n+1}}$$
$$=-\frac{\theta}{\Delta x^2}\left[\left(\frac{T_i^{n+1}+T_{i+1}^{n+1}}{2}\right)^{\alpha}+\frac{\alpha}{2}\left(\frac{T_i^{n+1}+T_{i+1}^{n+1}}{2}\right)^{\alpha-1}\left(T_{i+1}^{n+1}-T_i^{n+1}\right)\right], \quad (6\text{-}22)$$
$$for \quad i=1,...,I-1$$

According to Eqs. 3-4 and 5-28, the Jacobian matrix can also be approximately obtained similar as Eqs. 5-41 to 5-43.

For the sensitivity problem s_α, the same Jacobian matrix is used as the physical problem. The discretized residual function for the sensitivity problem is:

$$ress_i(\mathbf{s}^{n+1}) = \frac{s_i^{n+1} - s_i^n}{\Delta t} - \theta \cdot \left(\frac{\partial F}{\partial Y} s + \frac{\partial F}{\partial \alpha} \right)_i^{n+1} - (1-\theta) \cdot \left(\frac{\partial F}{\partial Y} s + \frac{\partial F}{\partial \alpha} \right)_i^{n}. \tag{6-23}$$

Although it is possible to directly evaluate the $\frac{\partial F}{\partial Y} s + \frac{\partial F}{\partial \alpha}$ term, the form becomes very complex and error-prone for $\frac{\partial F}{\partial \alpha}$ due to the complex form of $mms(x,t,\alpha)$ function (Eq. 6-6). This term can be approximated by Jacobian free method (Eq. 3-10) as

$$\left(\frac{\partial F}{\partial Y} s + \frac{\partial F}{\partial \alpha} \right)_i = \frac{F_i(x,t,\mathbf{T}+\sigma\cdot\mathbf{s},\alpha+\sigma) - F_i(x,t,\mathbf{T}-\sigma\cdot\mathbf{s},\alpha-\sigma)}{2\sigma}. \tag{6-24}$$

For the sensitivity problem for Δt in the first order scheme, Eqs 5-46 and 5-47 in the thermal wave problem are used since the time discretization scheme is exactly same.

6.3 Numerical Results for the Weak Nonlinear Diffusion Problem

6.3.1 Convergence Study for the Physical Problem

First we consider convergence studies for the physical problem. We run the problem from t=0 to t=10. Fig. 6-16 shows the space convergence study for the C-N scheme with a very small time step ($\Delta t = 10^{-4}$). The errors drop by about 4 times when Δx is halved, which clearly shows the 2nd order spatial step convergence rate. Fig. 6-17 shows the time convergence study for the C-N scheme with a small spatial step ($\Delta x = 1/640$). The solution errors drop by about four times when Δt is halved until the spatial error dominates the total error, which proves the 2nd order time step convergence rate. Fig. 6-18 shows the time convergence study for the C-N scheme with a very small spatial step ($\Delta x = 0.0001$). The secondary convergence range extends further down by two orders in this case. Fig. 6-19 shows the time convergence study for the 1st order backward Euler scheme with a small spatial step ($\Delta x = 1/640$). The solution errors drop approximately by half when Δt is halved until the spatial error dominates in the total numerical error, which shows the 1st order convergence rate. The spatial convergence rate is still 2nd order even for the 1st order time scheme.

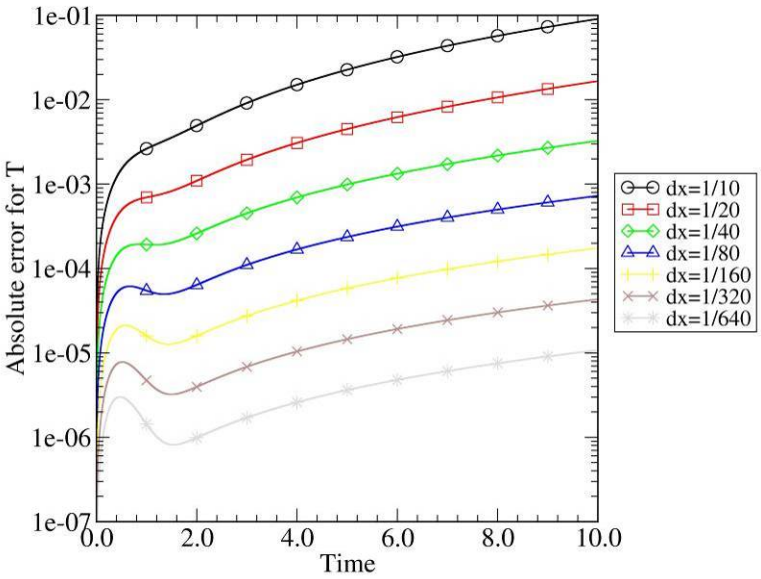

Figure 6-16: Space convergence study for the weak nonlinear diffusion problem, C-N scheme, $\Delta t = 10^{-4}$.

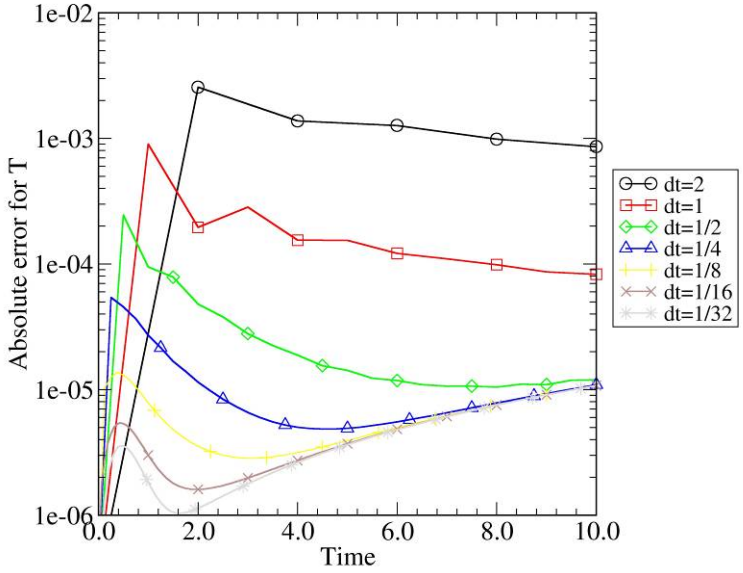

Figure 6-17: Time convergence study for the weak nonlinear diffusion problem, C-N scheme, $\Delta x = 1/640$.

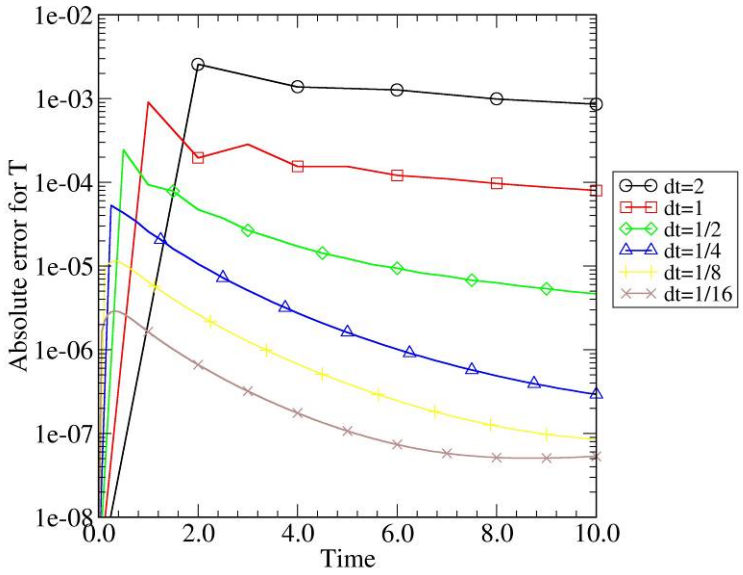

Figure 6-18: Time convergence study for the weak nonlinear diffusion problem, C-N scheme, Δx =1e-4.

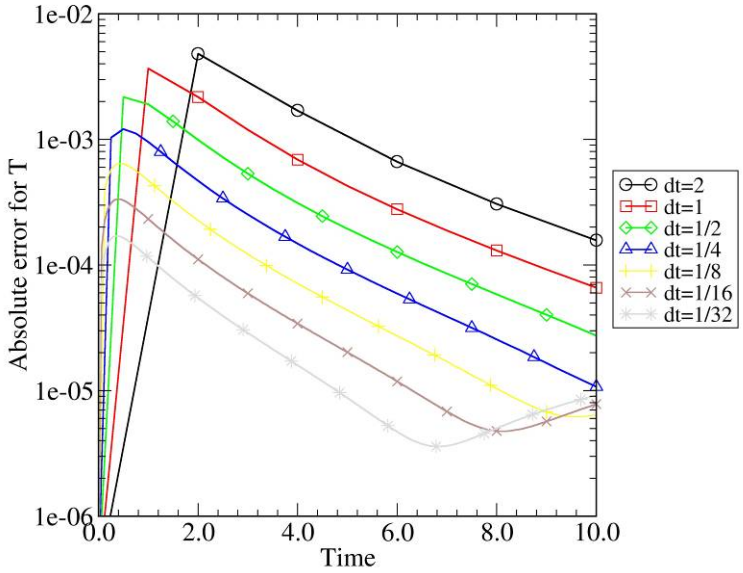

Figure 6-19: Time convergence study for the weak nonlinear diffusion problem, backward Euler scheme, Δx =1/640.

6.3.2 Convergence Study and Results for s_α

Fig. 6-20 shows the space convergence study for the sensitivity s_α for the C-N scheme with a very small time step ($\Delta t = 10^{-4}$). For time less than 2, we observe that there exists oscillation behavior with time. This may be due to the fact that the dynamical time scale

is 0 for time equal 0. 2nd order convergence speed is apparent for Δx. Fig. 6-21 shows the time convergence study for the sensitivity s_α for C-N scheme with a small spatial step (Δx =1/640). 2nd order convergence speed is achieved until Δt becomes too small when the spatial error begins to dominate. Fig. 6-22 shows the time convergence study for the sensitivity s_α for the 1st order backward Euler scheme with a small spatial step (Δx =1/640). It is very clear that the 1st order convergence speed is obtained.

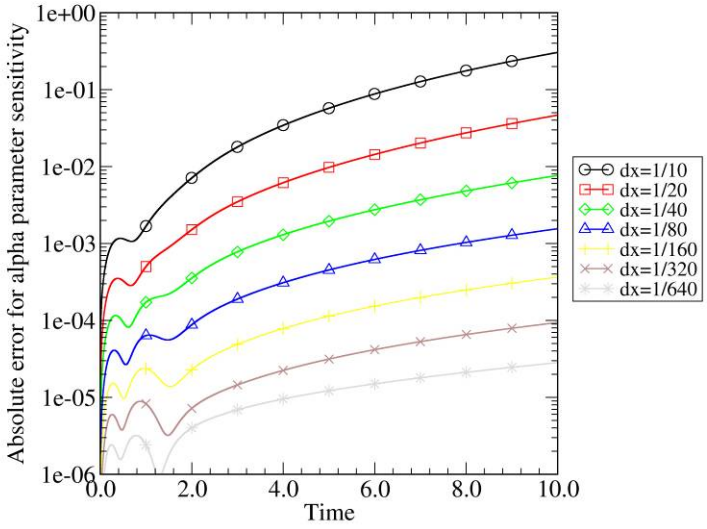

Figure 6-20: Space convergence study for the sensitivity s_α in the weak nonlinear diffusion problem, C-N scheme, Δt =10^{-4}.

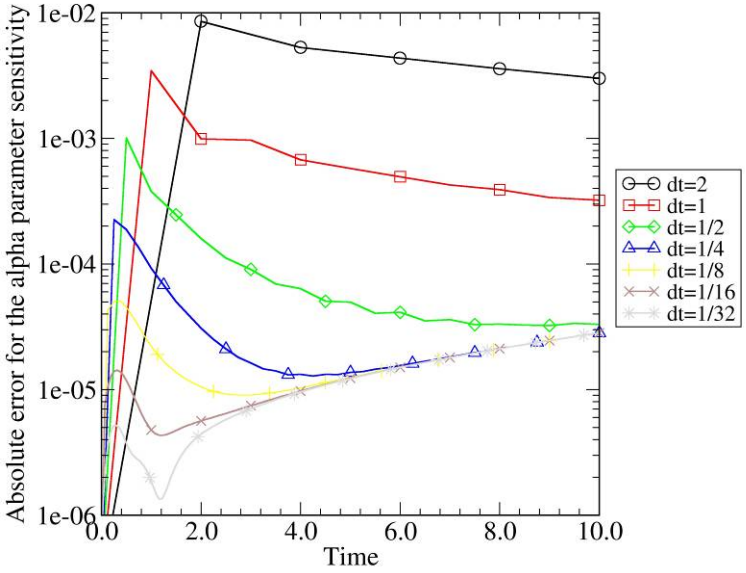

Figure 6-21: Time convergence study for the sensitivity s_α in the weak nonlinear diffusion problem, C-N scheme, Δx =1/640.

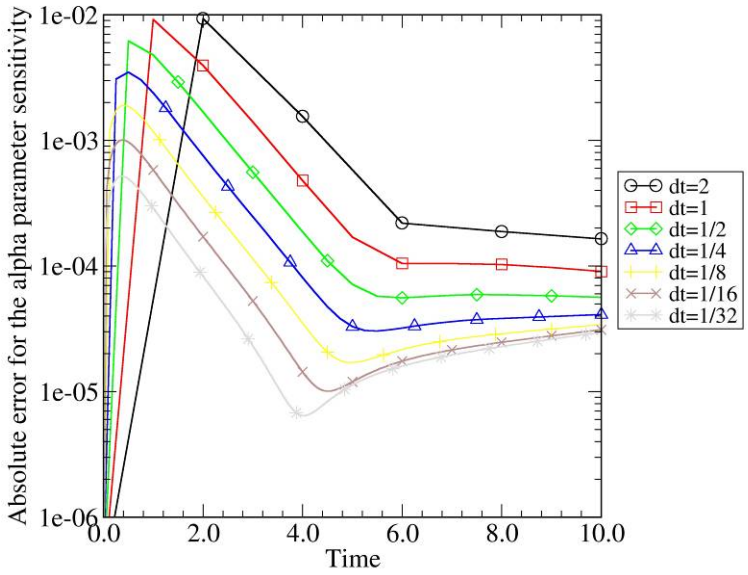

Figure 6-22: Time convergence study for the sensitivity s_α in the weak nonlinear diffusion problem, backward Euler scheme, Δx =1/640.

6.3.3 Time Step Sensitivity Convergence Study and Results

In this section, we investigate the time step sensitivity in the first order backward Euler scheme. The local truncation error term is same as Eq. (5-20):

$$LTE_t = \frac{\Delta t}{2}\frac{\partial^2 T}{\partial t^2}, \tag{6-25}$$

and the modified equation is

$$\frac{\partial T}{\partial t} - \frac{\Delta t}{2}\frac{\partial^2 T}{\partial t^2} = F(x,t,T,\alpha), \tag{6-26}$$

For this problem, we do not have an analytical solution for time step sensitivity $s_{\Delta t}$. Therefore 0 initial condition for $s_{\Delta t}$ will be used and we will check the correctness of $s_{\Delta t}$ solution by indirect method shown later. Similar to the thermal wave problem, an approximate numerical method and an analytical method are used to calculate $\frac{\partial F}{\partial \Delta t}$ as shown in Eq. (6-27) and Eq. (6-28), respectively:

$$\left(\frac{\partial F}{\partial \Delta t}\right)_i = \left(\frac{1}{2}\frac{\partial^2 T}{\partial t^2}\right)_i \approx \frac{1}{2\Delta t^2}\left(T_i^{n+1} + T_i^{n-1} - 2T_i^n\right), \tag{6-27}$$

$$\left(\frac{\partial F}{\partial \Delta t}\right)_i = \left(\frac{1}{2}\frac{\partial^2 T}{\partial t^2}\right)_i = -0.45\alpha^2 x_i^{\alpha t+1}\left(\ln x_i\right)^2. \tag{6-28}$$

From Fig. 6-19, we notice that the solution is not very sensitive with the time step and the time step error drops rapidly with time. Therefore, we are only interested in the early time evolution. Figs. 6-23 and 6-24 show the time step sensitivity $s_{\Delta t}$ for different time steps at time equal to 1, with analytical and numerical treatments on $\frac{\partial F}{\partial \Delta t}$, respectively. Both figures show that $s_{\Delta t}$ approaches to a curve with the decrease of Δt: Fig. 6-23 showing downward convergence direction and Fig. 6-24 showing upward convergence direction. Fig. 6-24 also shows that the time step sensitivity results have larger errors for very large Δt when the approximate numerical treatment of $\frac{\partial F}{\partial \Delta t}$ is used (Eq. 6-27). Fig. 6-25 compares the time step sensitivities from two different treatments on $\frac{\partial F}{\partial \Delta t}$ for a small time step. The results are very close. Therefore for a smaller time step, numerical treatment of $\frac{\partial F}{\partial \Delta t}$ can give a good time step sensitivity result.

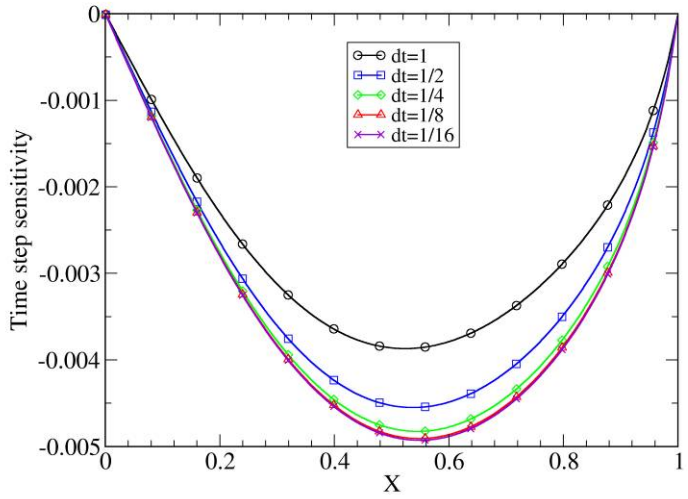

Figure 6-23: Time step sensitivity $s_{\Delta t}$ in the weak nonlinear diffusion problem, backward Euler scheme, Δx =1/640, t=1, with analytical treatment of $\frac{\partial F}{\partial \Delta t}$.

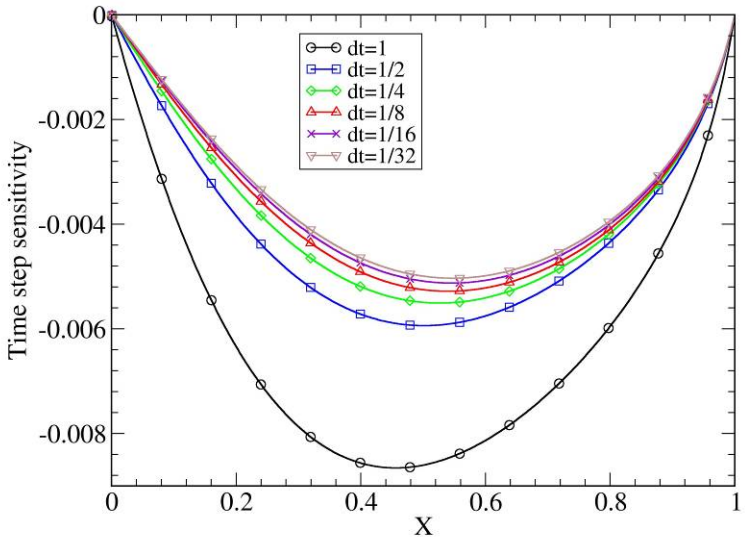

Figure 6-24: Time step sensitivity $s_{\Delta t}$ in the weak nonlinear diffusion problem, backward Euler scheme, Δx =1/640, t=1, with numerical treatment of $\frac{\partial F}{\partial \Delta t}$.

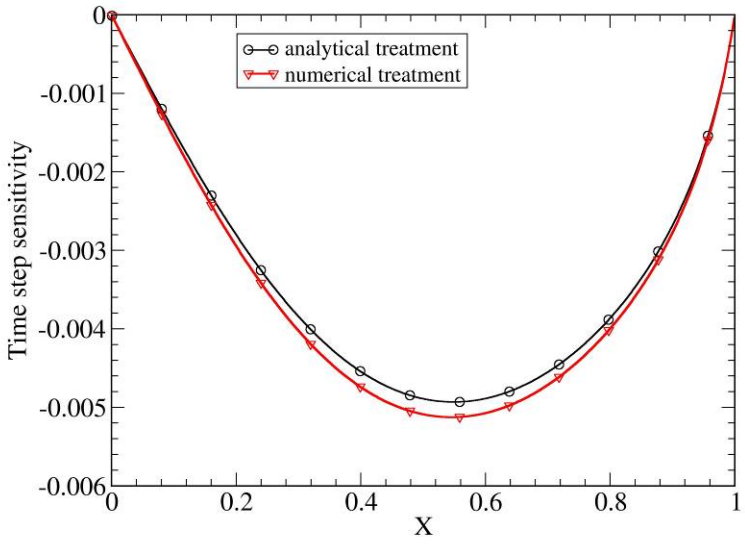

Figure 6-25: Comparison of time step sensitivity $s_{\Delta t}$ in the weak nonlinear diffusion problem from numerical and analytical treatment of $\frac{\partial F}{\partial \Delta t}$, backward Euler scheme, Δx =1/640, Δt=1/16, t=1.

Fig. 6-26 shows the spatial step convergence study result for $s_{\Delta t}$. Since we do not have analytical solution for $s_{\Delta t}$, a Richardson extrapolation method is used to estimate the space error. First a fine resolution result is obtained by setting Δx =1/640 and Δt=0.01.

Then the time step is fixed at 0.01 and spatial steps are decreased from 1/10 to 1/320. The time step sensitivity error is calculated by assuming the fine resolution result being the accurate solution. Overall error dynamical behavior demonstrates the 2nd order convergence speed.

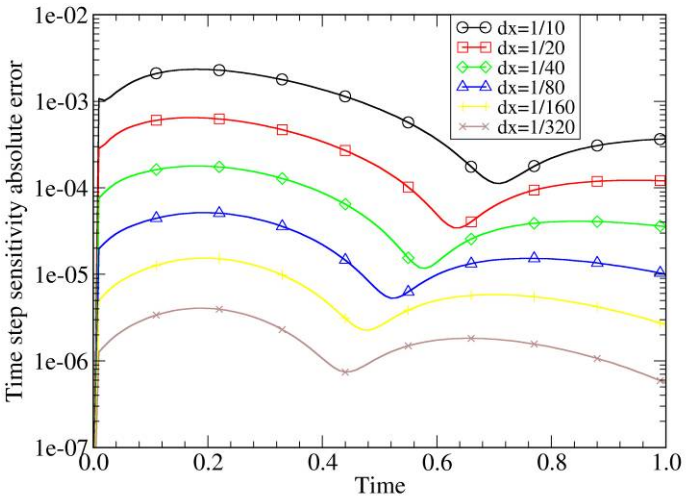

Figure 6-26: Space convergence study for the sensitivity $s_{\Delta t}$ in the weak nonlinear diffusion problem with analytical treatment of $\frac{\partial F}{\partial \Delta t}$, backward Euler scheme, Δt=0.01.

Fig. 6-27 shows an indirect check on the correctness of the calculated $s_{\Delta t}$ and how to use it. Because all the numerical solutions in this particular problem are not very sensitive to the time step, a zoom-in view is shown here. In this figure, the solid diamond line is the analytical solution at time equal to 1. The cross line is the numerical result with a time step of 0.5, a large time step but still smaller than the minimum dynamical time scale, which is the reference time step. The circle line is the numerical result with the reference time step reduced by 99%. We can take these two lines as time step convergence study with time steps reduced from 0.5 to 0.005. We can see the smaller time step generates a solution almost exactly the same as the analytical solution. The triangle line is calculated with Eq. 2-19 according to the numerical solution with the reference Δt=0.5 and its corresponding $s_{\Delta t}$. Note that the estimated solution according to the time step sensitivity is very close to the analytical solution or numerical solution with a much smaller time step. The fact implies the following three important points: (1) the time step sensitivity analysis is correct; (2) the accumulated temporal error can be estimated according to the time step sensitivity analysis method, i.e., about 0.4% for Δt=0.5 in this case; (3) the time step sensitivity analysis could play the same role as the time step convergence study and the potential computational saving is large since one can avoid the costly computation with series of smaller time steps.

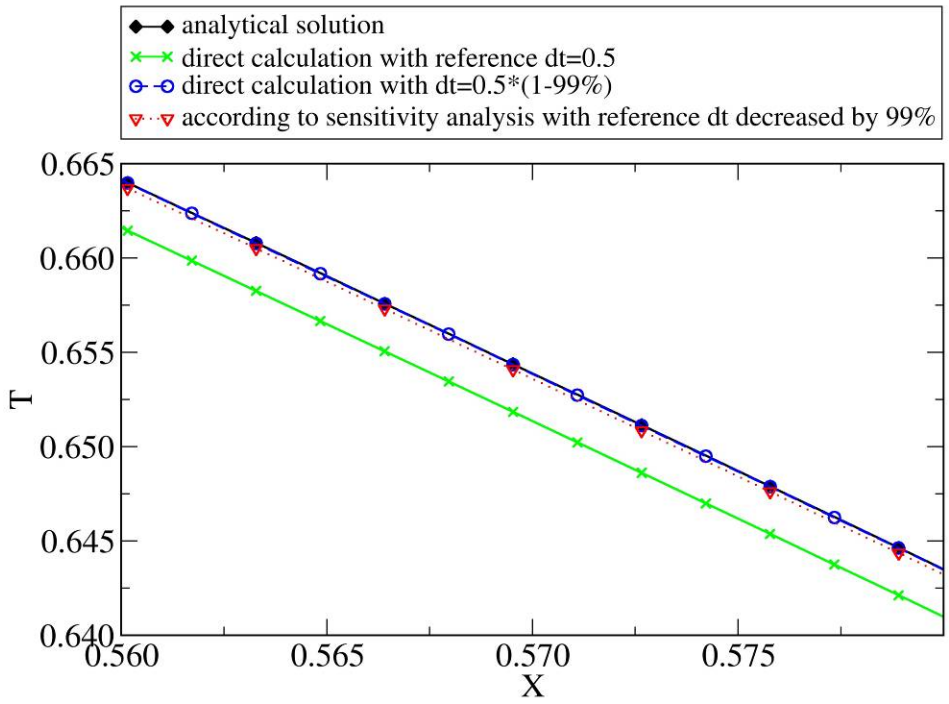

Figure 6-27: Comparison of analytical solution, direct time convergence study, and numerical error bars from sensitivity analysis result in the weak nonlinear diffusion problem, backward Euler scheme, Δx =1/640, time at 1.

6.3.4 Sensitivity Comparison

When all the parameter sensitivity solutions are available, a systematic comparison of parameter sensitivities can be performed. Fig. 6-28 compares sensitivity $s_{\Delta t}$ and s_{α} at t=0.1 and t=1. The solid lines are for time at 0.1 and the dash lines are for time at 1. Lines with circle symbols are $s_{\Delta t}$; and lines with diamond symbols are s_{α}. s_{α} is always much larger than $s_{\Delta t}$ for different time.

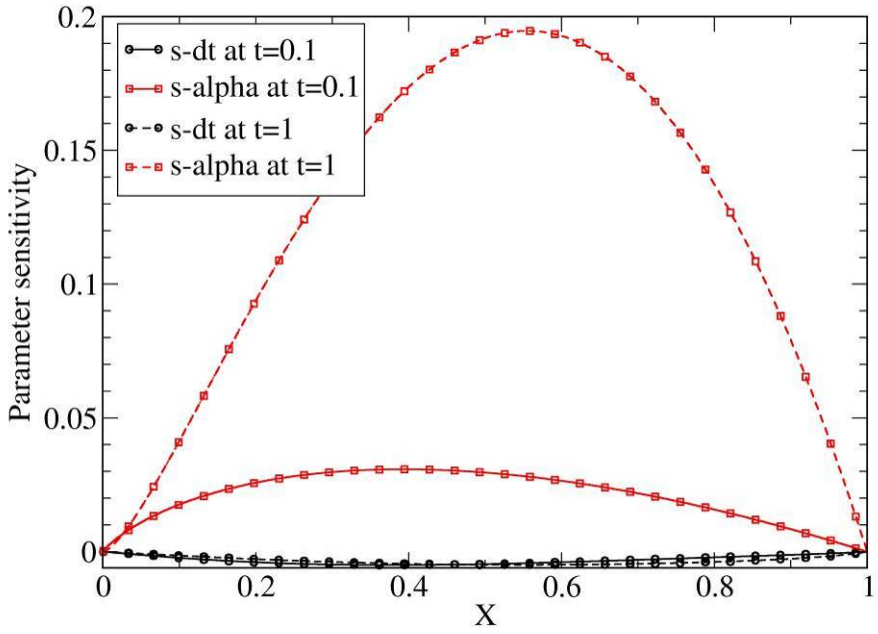

Figure 6-28: Comparison of sensitivity $s_{\Delta t}$ and s_{α} at t=0.1 and t=1 in the weak nonlinear diffusion problem, backward Euler scheme, Δx =1/640, Δt =0.01.

Figs. 6-29 and 6-30 compares the sensitivity analysis results from the forward sensitivity analysis method (shown as dash lines) and from direct calculations (shown as discrete points) by changing α by ±20%, at time 1 and 10, respectively. The forward sensitivity results match the direct calculation results very well. Note that the forward sensitivity only requires one run while the direct calculations require three runs.

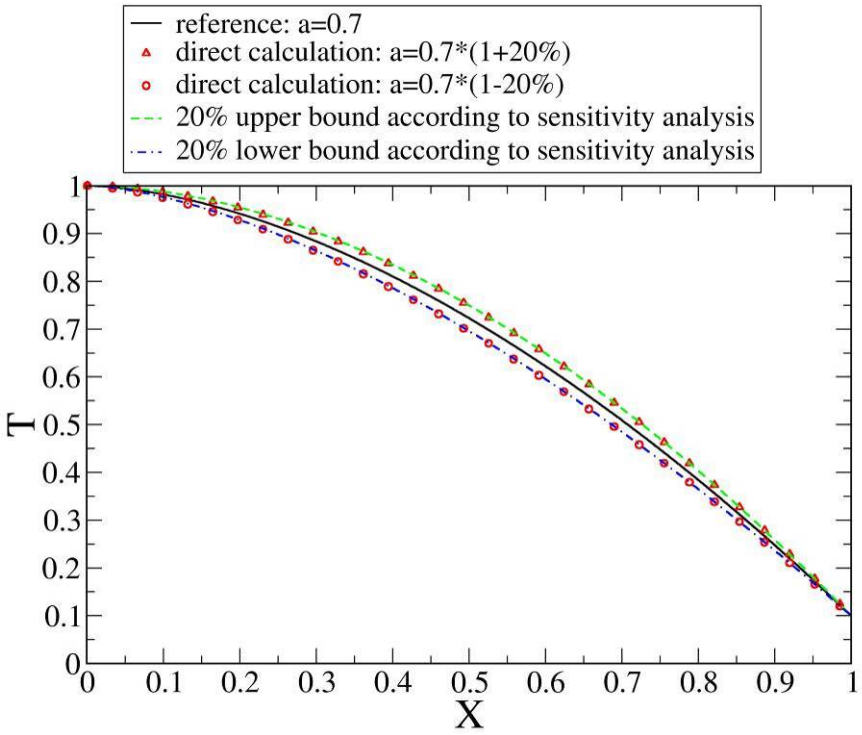

Figure 6-29: Comparison of sensitivity analyses for α between forward sensitivity analysis and direct calculation in the weak nonlinear diffusion problem, t=1, Δx =1/640, Δt =0.01, C-N scheme, uncertainty range: ±20%.

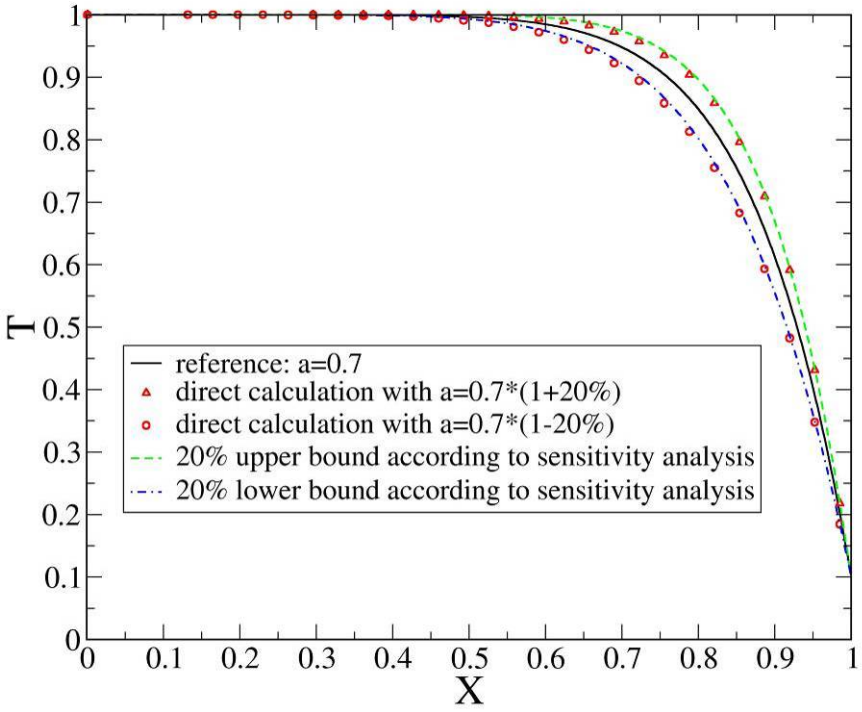

Figure 6-30: Comparison of sensitivity analyses for α between forward sensitivity analysis and direct calculation in the weak nonlinear diffusion problem, t=10, Δx =1/640, Δt =0.01, C-N scheme, uncertainty range: ±20%.

The extended forward sensitivity analysis provides a systematic method to evaluate the parameter sensitivity effects on solution, along with time and space convergence information. Fig. 6-31 compares sensitivity effects from the time step and α parameter for a large time step (Δt=1) at time equal to 1. Even for this large time step (remember that the minimum dynamical time scale at time equal 0 is about 2.3), the solution is much more sensitive to the physical parameter α than the time step. Fig. 6-32 shows the zoom-in view at time equal to 1. Fig. 6-33 shows similar result at time equal to 10. Fig. 6-34 shows the corresponding zoom-in view. Temporal errors in later time have been damped so that the physical parameter α sensitivity becomes more dominating. This case shows an example where closure models (reflected in the complex, strong, manufactured source term) play a major role while PDEs play a less important role. In conventional nuclear reactor system analysis codes, there exist evidences that such cases existing. In such situations, the simulation accuracy more depends on the accuracy of the closure model parameters than the PDEs. For these types of problems, even the solution is not very sensitive to the time step, knowing the fact is still very useful to have high confidence on the simulation results and save the computational cost.

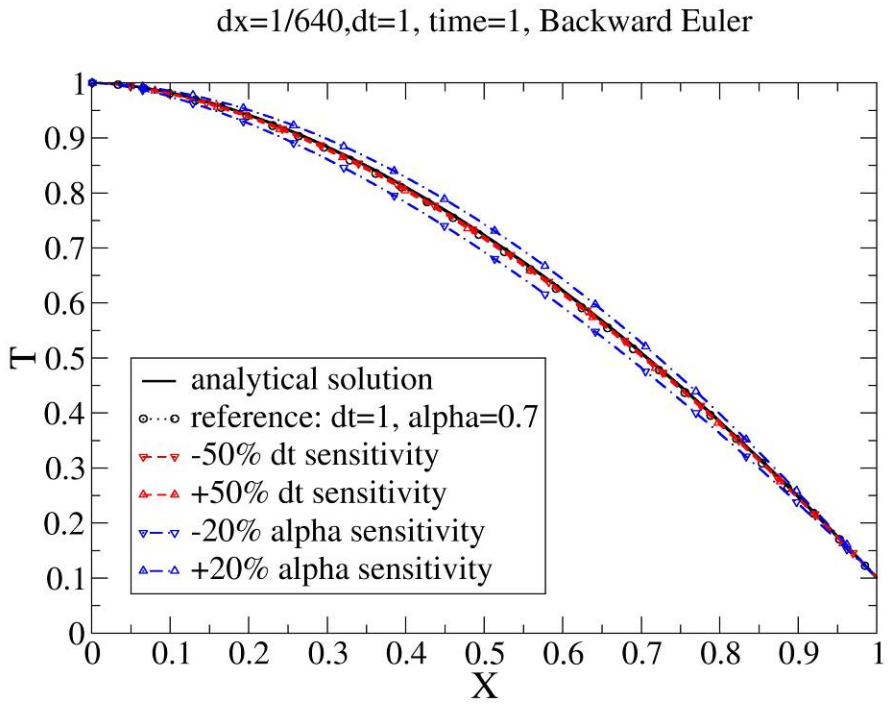

Figure 6-31: Comparison of sensitivity effects from time step and α in the weak nonlinear diffusion problem, t=1, backward Euler scheme, Δx =1/640, Δt =1.

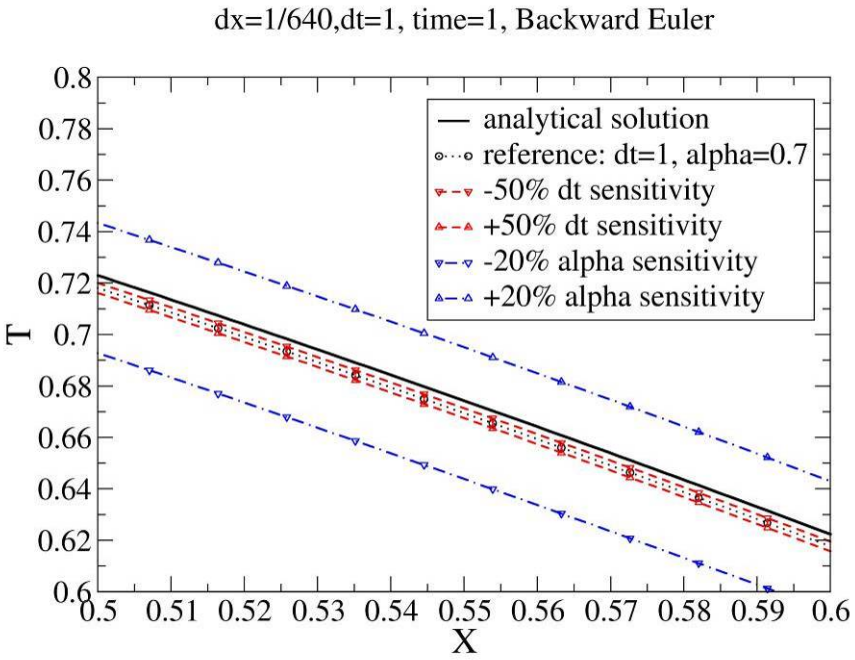

Figure 6-32: Comparison of sensitivity effects from time step and α (zoom-in view) in the weak nonlinear diffusion problem, t=1, backward Euler scheme, Δx =1/640, Δt =1.

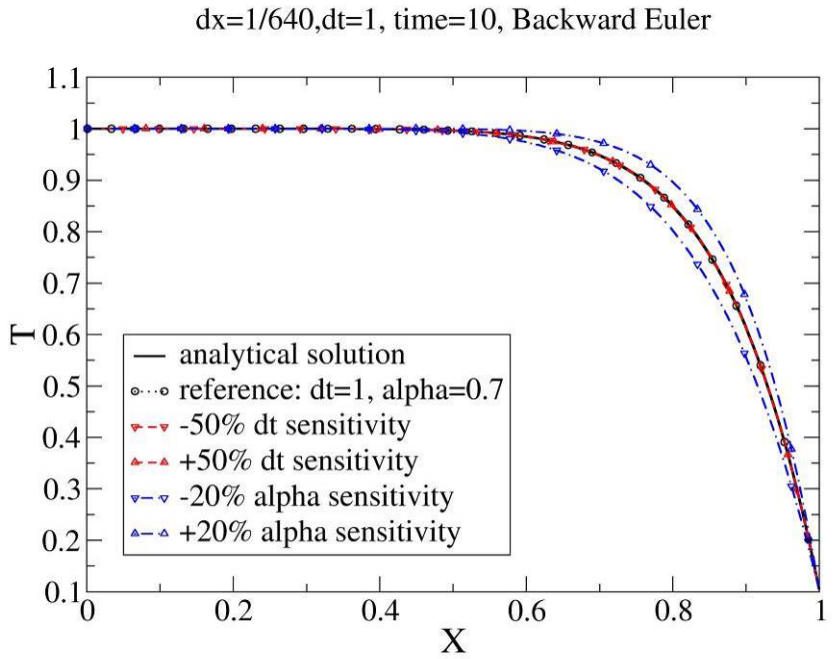

Figure 6-33: Comparison of sensitivity effects from time step and α in the weak nonlinear diffusion problem, t=10, backward Euler scheme, Δx =1/640, Δt =1.

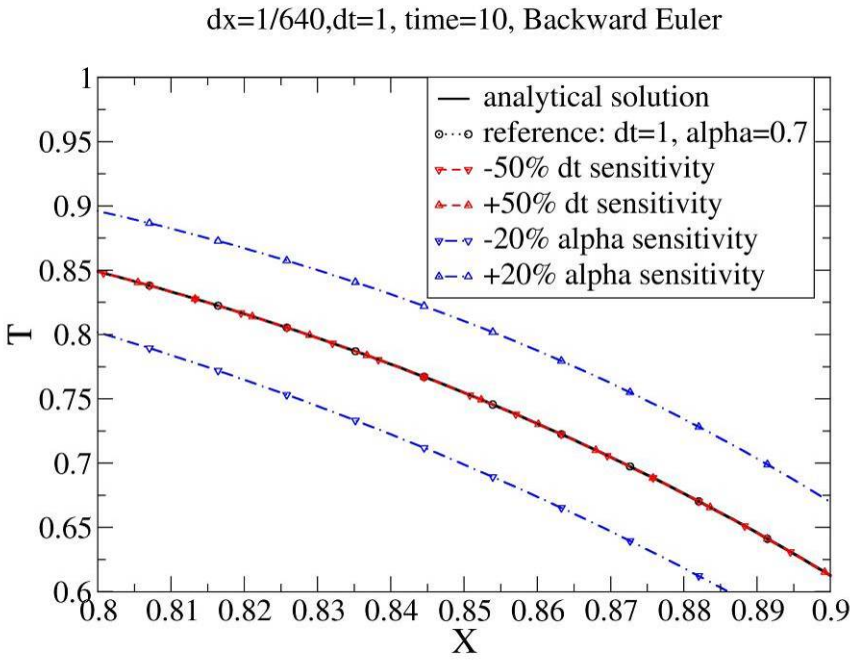

Figure 6-34: Comparison of sensitivity effects from time step and α (zoom-in view) in the weak nonlinear diffusion problem, t=10, backward Euler scheme, Δx =1/640, Δt =1.

6.4 Numerical Results for the Strong Nonlinear Diffusion Problem

6.4.1 Convergence Study for the Physical Problem

In this part, we discuss the strong nonlinear diffusion problem by setting α=7. First we consider convergence study for the physical problem. We run the problem from t=0 to t=1. Fig. 6-35 shows the space convergence study for C-N scheme with very small time step (Δt =10^{-4}). The errors drop by about 4 times when Δx is halved except for the first spatial step, which clearly shows the 2nd order spatial step convergence rate. As shown in Fig. 6-11, the minimum dynamical length scale becomes much smaller than 0.1 (the first spatial step) in later time. Therefore the first spatial step is out of asymptotic region for later time. Fig. 6-36 shows the time convergence study for the C-N scheme with a small spatial step (Δx =1/640). The solution errors drop by about four times when Δt is halved until the spatial error dominates the total error, which proves the 2nd order time step convergence rate. Fig. 6-37 shows the time convergence study for the 1st order backward Euler scheme with a small spatial step (Δx =1/640). The solution errors drop approximately by half when Δt is halved, which shows the 1st order convergence rate. The spatial convergence rate is still 2nd order even for the 1st order time scheme.

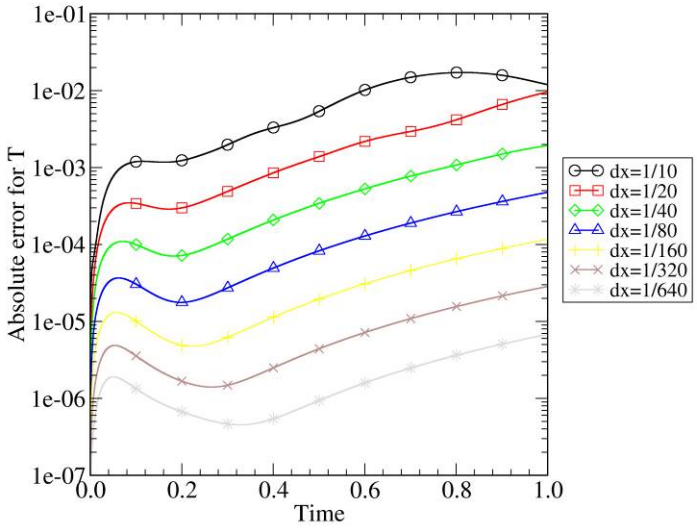

Figure 6-35: Space convergence study for the strong nonlinear diffusion problem, C-N scheme, $\Delta t = 10^{-4}$.

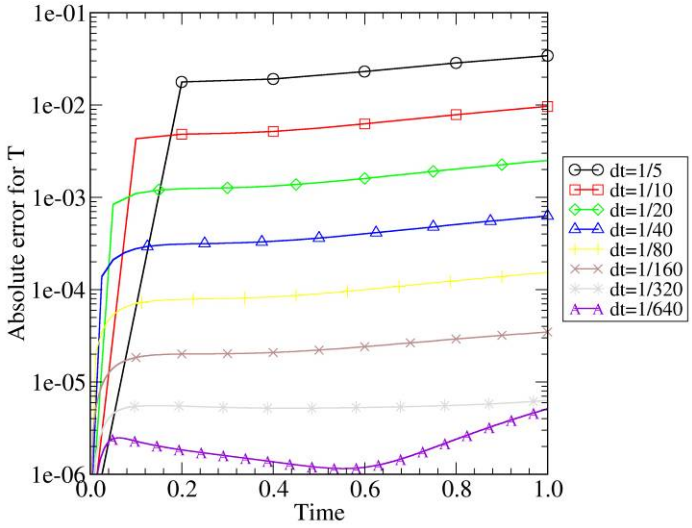

Figure 6-36: Time convergence study for the strong nonlinear diffusion problem, C-N scheme, $\Delta x = 1/640$.

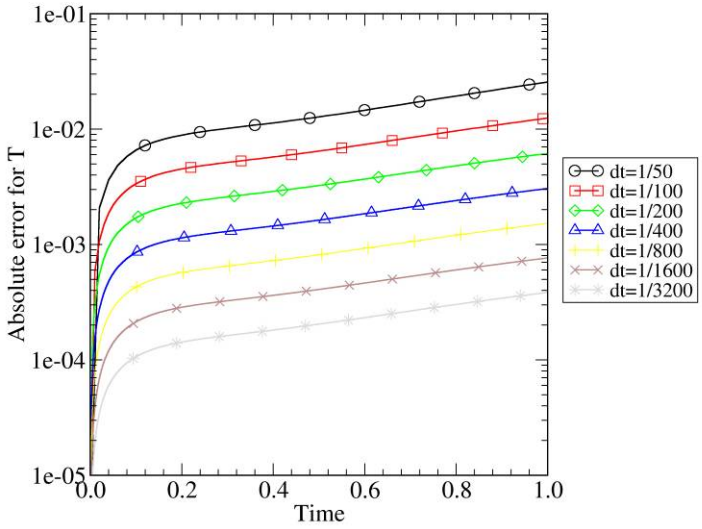

Figure 6-37: Time convergence study for the strong nonlinear diffusion problem, backward Euler scheme, Δx =1/640.

6.4.2 Convergence Study and Results for s_α

Fig. 6-38 shows the space convergence study for the sensitivity s_α for C-N scheme with very small time step ($\Delta t = 10^{-4}$). For time less than 0.2, we observe there exists oscillation behavior of error with time. This may due to very small time scale when time close to 0 and very small length scale for regions close to left and right boundaries. 2nd order convergence speed is apparent for smaller Δx until the time step error begins to dominate. Fig. 6-39 shows the time convergence study for the sensitivity s_α for the C-N scheme with a small spatial step (Δx =1/640). 2nd order convergence speed is achieved until Δt becomes too small when the spatial error begins to dominate. Fig. 6-40 shows the time convergence study for the sensitivity s_α for the 1st order backward Euler scheme with a small spatial step (Δx =1/640). It is very clear that the 1st order convergence speed is obtained.

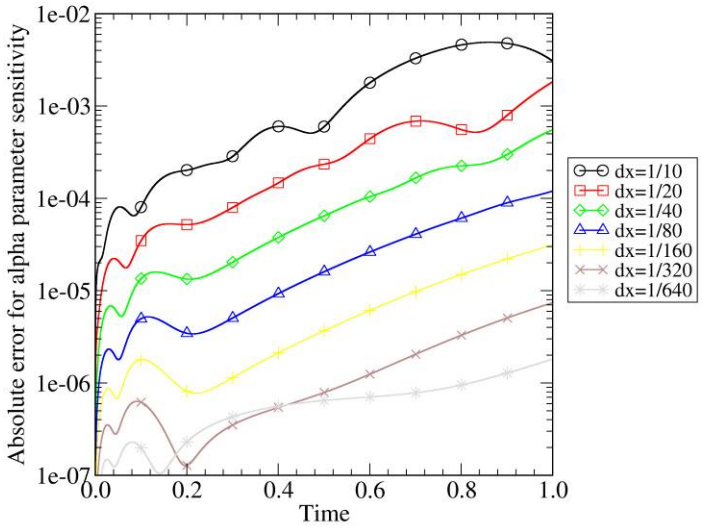

Figure 6-38: Space convergence study for the sensitivity s_α in the strong nonlinear diffusion problem, C-N scheme, $\Delta t = 10^{-4}$.

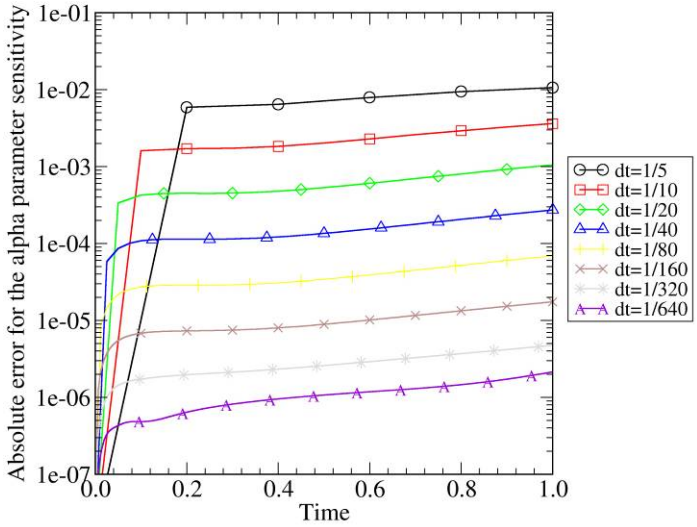

Figure 6-39: Time convergence study for the sensitivity s_α in the strong nonlinear diffusion problem, C-N scheme, $\Delta x = 1/640$.

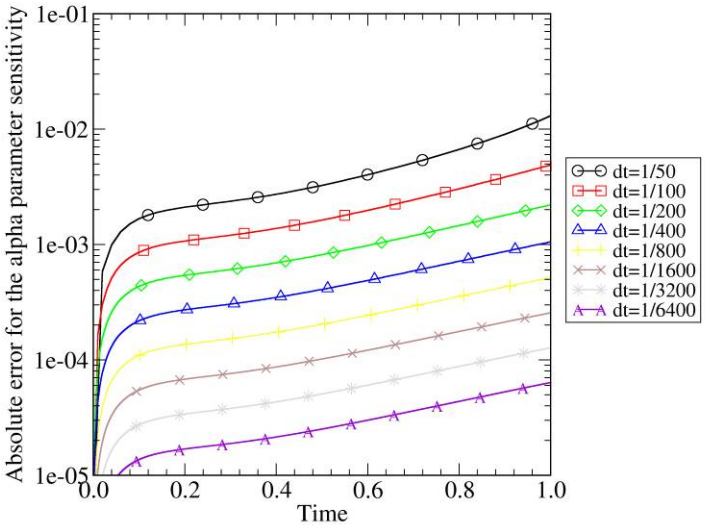

Figure 6-40: Time convergence study for the sensitivity s_α in the strong nonlinear diffusion problem, backward Euler scheme, Δx =1/640.

6.4.3 Time Step Sensitivity Convergence Study and Results

In this section, we investigate the time step sensitivity in the first order backward Euler scheme. Fig. 6-41 shows the time step sensitivity $s_{\Delta t}$ for different time steps at time equal to 1, with analytical treatment on $\frac{\partial F}{\partial \Delta t}$. It shows that $s_{\Delta t}$ approaches to a curve with the decrease of Δt.

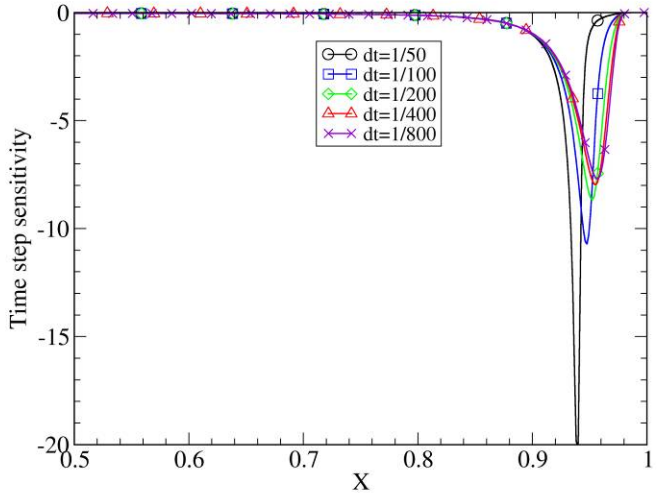

Figure 6-41: Time step sensitivity $s_{\Delta t}$ in the strong nonlinear diffusion problem, backward Euler scheme, Δx =1/640, t=1, with analytical treatment of $\frac{\partial F}{\partial \Delta t}$.

Fig. 6-42 shows the spatial step convergence study result for $s_{\Delta t}$. Since we do not have analytical solution for $s_{\Delta t}$, a Richardson extrapolation method is used to estimate the space error. First a fine resolution result is obtained by setting Δx=1/640 and Δt=0.001. Then the time step is fixed at 0.001 and spatial steps are increased from 1/10 to 1/320. The time step sensitivity error is calculated by assuming the fine resolution result being the accurate solution. Overall error dynamical behavior shows the 2nd order convergence speed for smaller Δx.

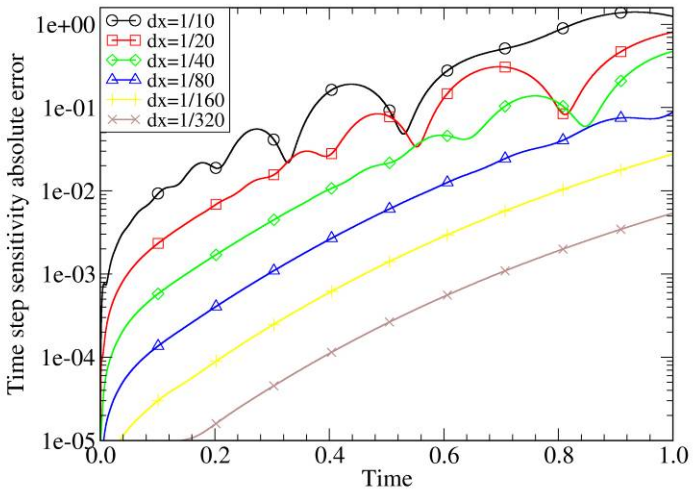

Figure 6-42: Space convergence study for the sensitivity $s_{\Delta t}$ in the strong nonlinear diffusion problem with analytical treatment of $\frac{\partial F}{\partial \Delta t}$, backward Euler scheme, Δt=0.001.

Fig. 6-43 shows an indirect check on the correctness of the calculated $s_{\Delta t}$ and how to use it. Because all the numerical solutions in this particular problem are not very sensitive to the time step, a zoom-in view is shown here. In this figure, the solid diamond line is the analytical solution at time equal to 1. The cross line is the numerical result with a time step of 0.005, a relative large time step for this strong nonlinear problem, which is the reference time step. The circle line is the numerical result with the reference time step reduced by 90%. We can take these two lines as the time step convergence study with the time step being reduced from 0.005 to 0.0005. We can see the smaller time step generates a solution very close to the analytical solution. The triangle line is calculated with Eq. 2-19 according to the numerical solution with the reference Δt=0.005 and its corresponding $s_{\Delta t}$. Note that the estimated solution according to the time step sensitivity is quite close to the analytical solution or numerical solution with a much smaller time step. Similar to the weak nonlinear diffusion problem, the fact implies the following three important points: (1) the time step sensitivity analysis is correct; (2) the maximum accumulated temporal error can be estimated according to the time step sensitivity

analysis method, i.e., about maximum 10% error for Δt =0.005 in this case; (3) the time step sensitivity analysis could play the same role as the time step convergence study and the potential computational saving is large since one can avoid the costly computation with small time steps.

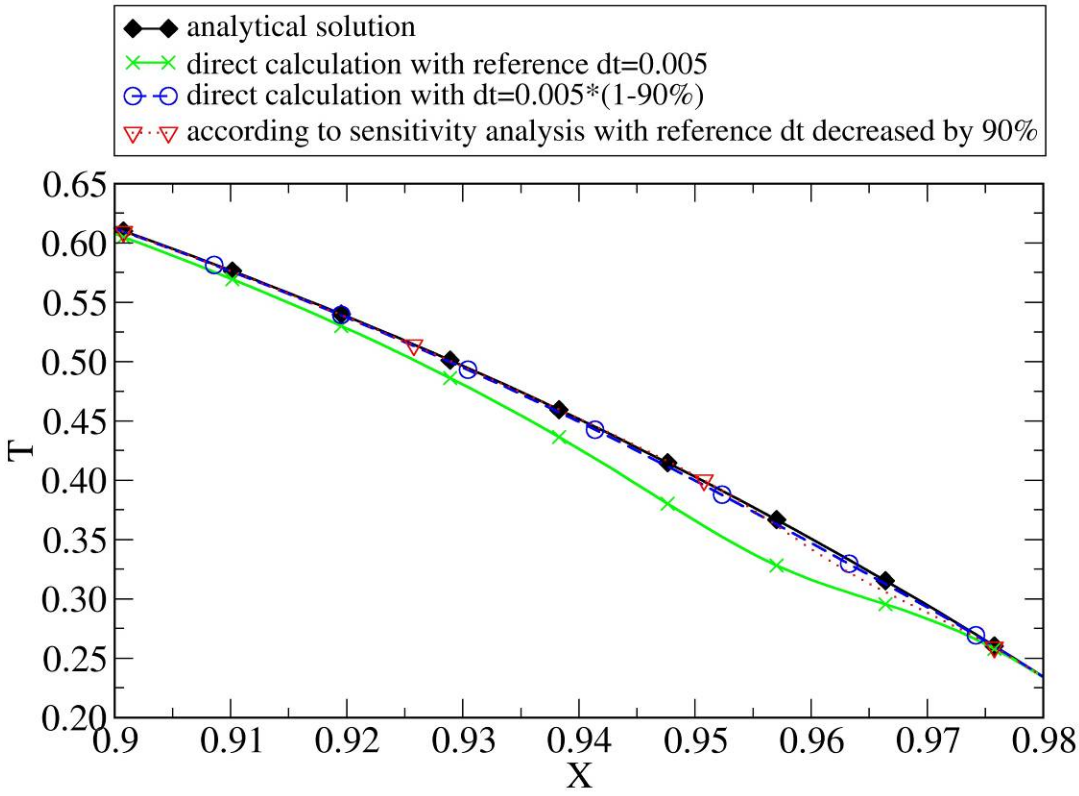

Figure 6-43: Comparison of analytical solution, direct time convergence study, and numerical error bars from sensitivity analysis result in the strong nonlinear diffusion problem, backward Euler scheme, Δx =1/640, time at 1.

6.4.4 Sensitivity Comparison

When all the parameter sensitivity solutions are available, a systematic comparison of parameter sensitivities can be performed. Fig. 6-44 compares sensitivity $s_{\Delta t}$ and s_α at t=0.1 and t=1. The solid lines are for time at 0.1 and the dash lines are for time at 1. Lines with circle symbols are $s_{\Delta t}$; and lines with diamond symbols are s_α. $s_{\Delta t}$ is always larger than s_α for different time and the order of $s_{\Delta t}$ increases rapidly with time.

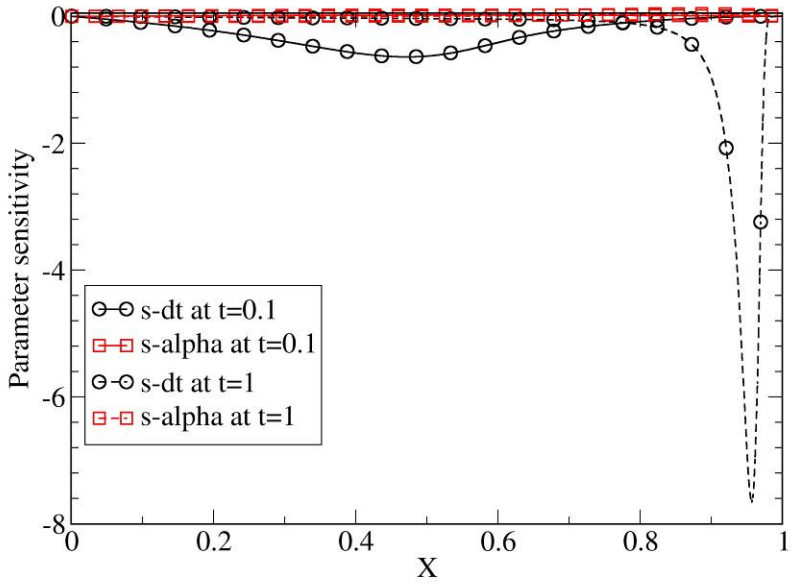

Figure 6-44: Comparison of sensitivity $s_{\Delta t}$ and s_{α} at t=0.1 and t=1 in the strong nonlinear diffusion problem, backward Euler scheme, Δx =1/640, Δt =0.001.

Fig. 6-45 compares the sensitivity analysis results from the forward sensitivity analysis method (shown as dash lines) and from direct calculations (shown as discrete points) by changing α by ±20%, at time 1. The forward sensitivity results match the direct calculation results very well.

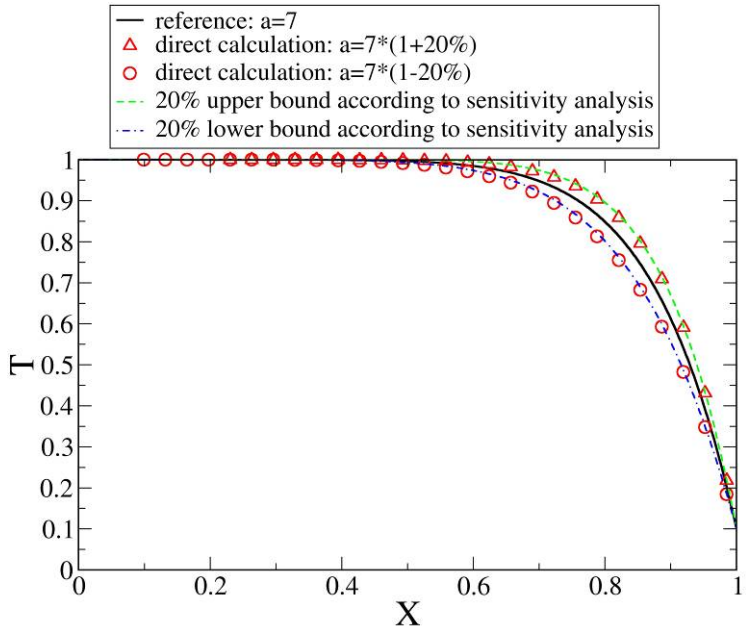

Figure 6-45: Comparison of sensitivity analyses for α between forward sensitivity analysis and direct calculation in the strong nonlinear diffusion problem, t=1, Δx =1/640, Δt =0.001, C-N scheme, uncertainty range: ±20%.

The extended forward sensitivity analysis provides a systematic method to evaluate the parameter sensitivity effects on solution, along with time and space convergence information. Fig. 6-46 compares sensitivity effects from time step and α parameter for a relative large time step (Δt=0.01) at time equal to 1. Fig. 6-47 shows the zoom-in view at time equal to 1. The solution is more sensitive to the physical parameter α than the time step in majority of the computational domain. However, the time step uncertainty bar has same order of width as the physical parameter α uncertainty bar in a small region close to the right boundary, where exists large numerical error. The local numerical error has been correctly captured by the time step sensitivity analysis. Actually, the -90% Δt bar corrects the numerical error so successfully that the lower time step uncertainty bar is very close to the analytical solution.

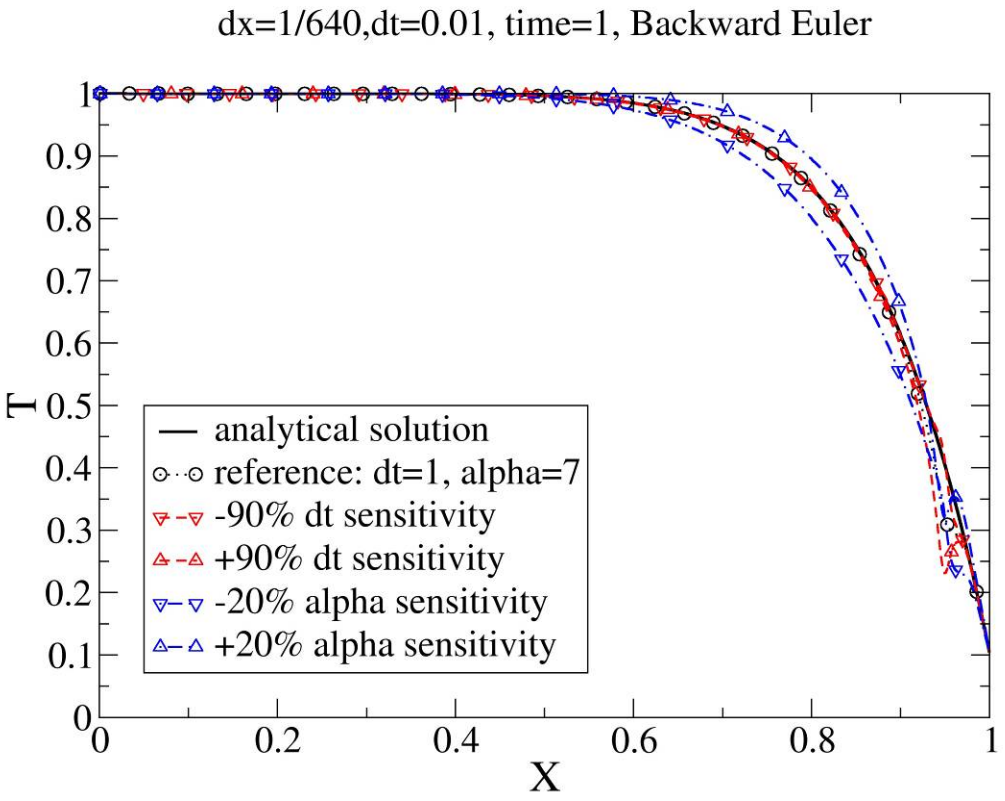

Figure 6-46: Comparison of sensitivity effects from time step and α in the strong nonlinear diffusion problem, t=1, backward Euler scheme, Δx =1/640, Δt =0.01.

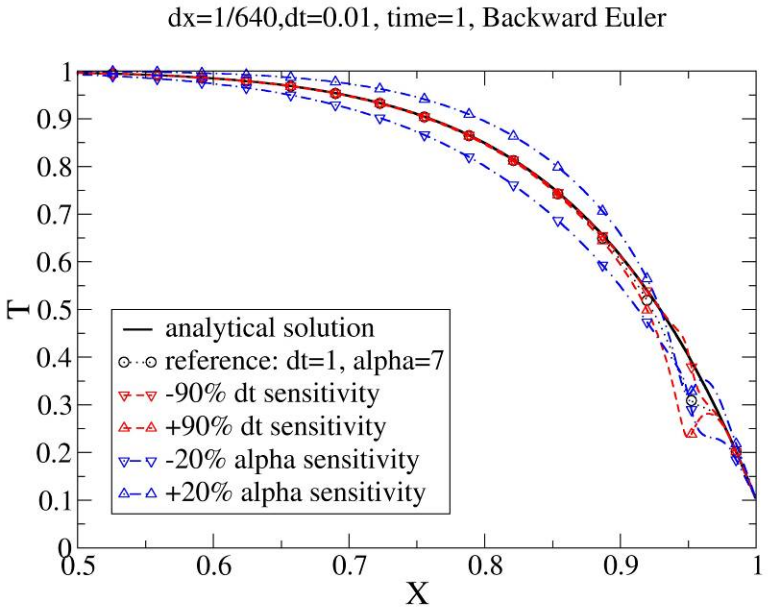

Figure 6-47: Comparison of sensitivity effects from time step and α (zoom-in view) in the strong nonlinear diffusion problem, t=1, backward Euler scheme, Δx =1/640, Δt =0.01.

Fig. 6-48 shows similar result at time equal to 1 for a small time step (Δt=0.001). In this case, the solution is not sensitive to the time step; therefore the solution and sensitivity results are reliable.

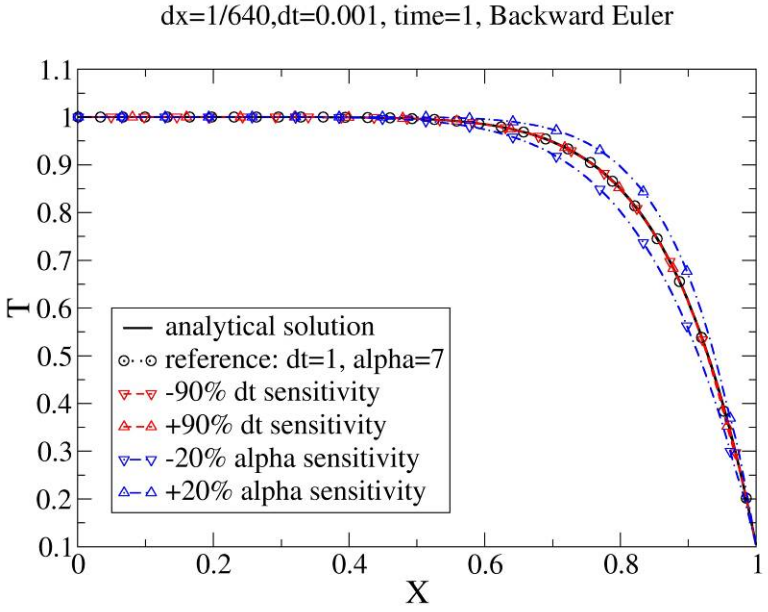

Figure 6-48: Comparison of sensitivity effects from time step and α in the strong nonlinear diffusion problem, t=1, backward Euler scheme, Δx =1/640, Δt =0.001.

7. SUMMARY

Applying the extended forward sensitivity analysis method to two benchmark problems shows the correctness, efficiency, and large potential to extend the method to more general systems. By taking advantage of intimate knowledge of the simulation code, this "glass box" method can generate similar sensitivity information as the conventional "black box" approach with couples of runs to cover a large uncertainty region. Therefore, the computational saving potential is very large. Forward sensitivity method is simple in mathematics and can be relatively easy to implement in a large code by adding sensitivity equation residues along with the physical problem residues. The formed computation structures are naturally suitable for parallel computation.

By extending the forward sensitivity method to include time and spatial steps as special parameters, numerical errors can be quantified against other physical parameters. This extension makes the forward sensitivity method a much more powerful tool to help uncertainty analysis. By knowing the relative sensitivity of time and space steps with other interested physical parameters, the simulation is allowed to run at appropriate time and space steps without affecting the confidence to the physical parameter sensitivity results.

Two well defined benchmark problems, thermal wave and nonlinear diffusion, are utilized to demonstrate the extended forward sensitivity analysis. All the physical solutions, parameter sensitivity solutions, even time step sensitivity in one case, have analytical forms, which allows the verification to be done in the strictest sense. A pilot code, Extended Forward sensitivity analysis pilot code (EFA), has been developed to implement the above work. While V&V has been widely recognized as indispensable to high fidelity simulation, very few of practical works have been pursued to quantify numerical error sensitivity along with physical parameter sensitivities. The extended forward sensitivity method can potentially fill the gap.

The work described in this report is preliminary and future works are necessary to apply this method into a large system code. Few examples include: (1) extend the method for spatial step sensitivity; (2) identify or design new verification problems with different natures to further verify the feasibility of the extended forward sensitivity analysis; (3) extend the work to multiple equation systems and multiple component systems.

ACKNOWLEDGEMENT

This work was supported through INL Laboratory Directed Research and Development program under DOE Idaho Operations Office Contract DE-AC07-05ID14517.

REFERENCE

1. W.L. Oberkampf and T.G. Trucano, "Verification and Validation in Computational Fluids Dynamics," *Progress in Aerospace Sciences*, **Vol. 38**, pp. 209-272 (2002).
2. R.B. Bond, et. al., "Manufactured Solution for Computational Fluid Dynamics Boundary Condition Verification," *AIAA Journal*, **Vol. 45**, No. 9, pp. 2224-2236 (2007).
3. M.D. Tocci, "Sensitivity Analysis of Large-Scale Time Dependent PDEs," *Applied Numerical Mathematics*, **Vol. 37**, pp. 109-125 (2001).
4. S.L. Lee, C.S. Woodward, F. Graziani, "Analyzing Radiation Diffusion Using Time-Dependent Sensitivity-Based Techniques," *Journal of Computational Physics*, **Vol. 192**, pp. 211-230 (2003).
5. K.J. Dowding, B.F. Blackwell, "Sensitivity Analysis for Nonlinear Heat Conduction," *Journal of Heat Transfer*, **Vol. 123**, pp. 1-10 (2001).
6. A.C. Hindmarsh, et. al., "SUNDIALS: Suite of Nonlinear and Differential/Algebraic Equation Solvers," *ACM Transactions on Mathematical Software*, **Vol. 31**, No. 3, pp. 363-396 (2005).
7. L.P. Pagani, G.E. Apostolakis, and P. Hejzlar, "The Impact of Uncertainties on the Performance of Passive Systems," *Nuclear Technology*, **Vol. 149**, pp. 130-140 (2005).
8. P. Vinai et al., "A Statistical Methodology for Quantification of Uncertainty in Best Estimate Code Physical Models," *Annals of Nuclear Energy*, **Vol. 34**, pp. 628-640 (2007).
9. Y. Cao and L. Petzold, "A Posteriori Error Estimation and Global Error Control for Ordinary Differential Equations," SIAM Journal of Scientific Computing, Vol. 26, No.2, pp. 359-374 (2004).
10. D.G. Cacuci and M. Ionescu-Bujor, "Adjoint Sensitivity Analysis of the RELAP5/MOD3.2 Two-Fluid Thermal-Hydraulic Code System-I: Theory," *Nuclear Science and Engineering*, **Vol. 136**, pp. 59-84 (2000).
11. D.G. Cacuci, *Sensitivity and Uncertainty Analysis*, Chapman & Hall/CRC, ISBN 1-58488-115-1 (2003).
12. D.A. Knoll and D.E. Keyes, "Jacobian-Free Newton-Krylov Methods: A Survey of Approaches and Applications," *Journal of Computational Physics*, **Vol. 193**, No. 2, pp. 357-397 (2004).
13. V.A. Mousseau, "A Fully Implicit Hybrid Solution Method for a Two-Phase Thermal-Hydraulic Model," *Journal of Heat Transfer*, **Vol. 127**, pp. 531-539 (2005).
14. D.A. Knoll, L. Chacon, L.G. Margolin, and V.A. Mousseau, "On balanced approximations for time integration of multiple time scales systems," *Journal of Computational Physics*, **Vol. 185**, pp.583-611, (2003).
15. O. Knio, H. Najm, P. Wyckoff, "A Semi-implicit Numerical Scheme for Reacting Flow: II. Stiff Operator-split Formulation," *Journal of Computational Physics*, **Vol. 154**, pp. 428-467 (1999).
16. V.S. Mahadeven and J.C. Ragusa, "Coupling Schemes for Multiphysics Reactor Simulation," Idaho National Laboratory external report, INL/EXT-07-13490 (2007).